ANODIC POLARISATION BEHAVIOUR OF COPPER IN CHLORIDE AND BROMIDE SOLUTIONS CONTAINING BENZOTRIAZOLE, TOLYLTRIAZOLE, AND METHYLBENZIMIDAZOLE

by

TERENCE JOHN ABEN

B.A.Sc., The University of British Columbia, 1991

A THESIS SUBMITTED IN PARTIAL FULFILLMENT OF THE REQUIREMENTS

FOR THE DEGREE OF

MASTER OF APPLIED SCIENCE

in

THE FACULTY OF GRADUATE STUDIES

Department of Metals and Materials Engineering

We accept this thesis as conforming to the required standard.

THE UNIVERSITY OF BRITISH COLUMBIA

April 1997

In presenting this thesis in partial fulfilment of the requirements for an advanced degree at the University of British Columbia, I agree that the Library shall make it freely available for reference and study. I further agree that permission for extensive copying of this thesis for scholarly purposes may be granted by the head of my department or by his or her representatives. It is understood that copying or publication of this thesis for financial gain shall not be allowed without my written permission.

Department of Metals + Materials Engineering

The University of British Columbia
Vancouver, Canada

Date 4/24/97

Abstract

The interactions of oxide free copper surfaces with the organic chemicals benzotriazole, tolyltriazole and methylbenzimidazole were studied in solutions containing sodium chloride to elucidate the effect of modifying the molecular structure of benzotriazole on the inhibition of copper corrosion. All experiments were performed in solutions containing 1M NaCl. Experiments were performed using organic molecule concentrations of 8.39×10^{-3} M and 8.39×10^{-4} M and at pH values of 6.0 and 3.0.

Potentiodynamic polarisation studies were used to gather information that was then compared to the established potential-pH equilibria. Polarisation scan rates of 1 mV/s and 0.2 mV/s were used.

Inhibition of the anodic dissolution reactions was observed under all conditions studied using benzotriazole and tolyltriazole. The inhibition behaviour of benzotriazole and tolyltriazole are very similar and appear to use the same inhibition mechanism. Methylbenzimidazole was not found to produce an inhibiting effect.

The potential-pH (E-pH) diagram for the $Cu\text{-}Br^{-}\text{-}H_2O$ system was constructed from the available thermodynamic data. Polarisation scans were performed using copper in bromide solutions at pH 3.0 and 6.54 to confirm the behavioural predictions based on the E-pH diagram.

To confirm the inhibition model proposed by Tromans et al.[1] on the behaviour of benzotriazole on oxide free copper surfaces in chloride media, experiments were performed in solution containing bromide and benzotriazole to eliminate the possibility

of synergistic reactions with chloride, as well as to collaborate previous conclusions with a different set of thermodynamic data.

Potentiodynamic polarisation studies were used to gather information on the behaviour of benzotriazole and tolyltriazole in sodium bromide solutions at pH values of 3.0 and 6.0.

Table of Contents

Table of Figures

Table of Tables

Table of Equations

Acknowledgements

I would like to express my thanks to the Natural Sciences and Engineering Council of Canada for contributing financial support to this study. I would also like to thank the Keyes Foundation for the generous award of a postgraduate fellowship, also in support of this study.

I would like to thank my supervisor, Professor Desmond Tromans for the opportunity to perform this study, and for his encouragement, insights, and suggestions in support of this work.

I would like to thank my parents, John and Eleanor Aben, for their constant encouragement and influence throughout my life to learn, follow my interests, reach for higher goals, and believe that there are no limits to what can be achieved. It is these influences that stand at the core of what I am today.

I would like to express my gratitude to my fiancé, Jodi Duncan, for her patience, understanding, encouragement and motivation while writing this document. Above all, I thank her for being my reason to finish it.

Lastly, I would like to thank Michael O'Brien for his small but critical contribution to this thesis: setting deadlines. Without this it may have never been finished.

Chapter 1 Introduction

The anodic polarisation behaviour of copper in aqueous bromide solutions has received little attention in the literature whereas the behaviour of copper in chloride solutions has been the subject of several studies [1,2,3,4,5,6,7]. Both halides are known to form soluble cuprous complexes [8,9,10,11,12,13]. The greater degree of interest in the effect of chlorides in solution stems from the abundance of the chloride ion in nature. It is well established that the $CuCl_2^-$ species causes anodic dissolution of copper in acidic [2,4,5,6,7] and neutral chloride solutions [1,3] under potential (E) and pH conditions that would normally promote immunity of the metal or formation of a passive Cu_2O layer in the absence of chloride. This behaviour is consistent with the thermodynamic data and subsequent predictions arising from the E-pH equilibrium diagrams for the Cu-Cl^--H_2O [1].

The anodic dissolution of copper in chloride solutions exhibits apparent Tafel behaviour with a slope (dE / $d\log i$) of ~60 mV near 25 °C [1,3,4,5,6] that is dependent on the potential controlled concentration of $CuCl_2^-$ ions at the outer Helmholtz plane and the subsequent mass transport of these ions through the diffusion layer [3,5,6,7]. This process was described by Smyrl [5] as mass transport-kinetic control. If the cuprous bromide complex posses similar stability's to those of the chloride cuprous complexes a similar domain of aqueous dissolution should be found on the corresponding E-pH diagram for the Cu-Br^--H_2O system and the apparent Tafel behaviour should be observed during polarisation scans.

Benzotriazole is one of the most widely used agents for inhibiting corrosion of copper [14,15]. Beginning with the pioneering work of Cotton and co-workers [16,17] many

investigations relating to the inhibition phenomenon of benzotriazole have been published towards elucidating the mechanism of corrosion inhibition. These investigations have included electrochemical and corrosion studies in the presence and absence of benzotriazole [14,18,19,20,21,22,23,24,25], the adsorption behaviour of benzotriazole [21,25,26], and ellipsometric studies of corrosion films [14,27].

Benzotriazole (1H-benzotriazole) is a heterocyclic organic compound with the molecular formula $C_6H_4N_3H$ and a benzenoid structure shown below in Figure 1.

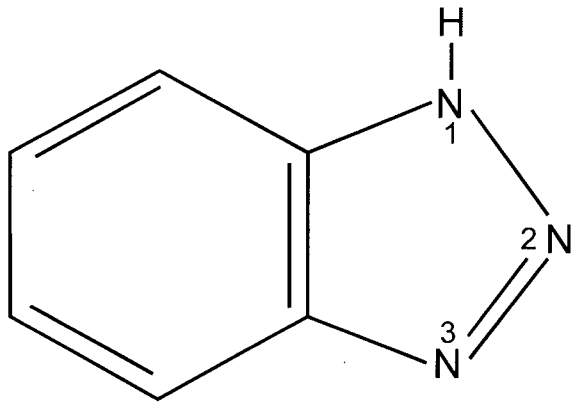

Figure 1 Molecular structure of benzotriazole

The compound exists in solution as a neutral benzenoid molecule $C_6H_4N_3H$ (BTAH), a dissociated anionic quinoid species $C_6H_4N_3$ (BTA^-), or as a protonated cationic quinoid species $C_6H_4N_3H_2$ ($BTAH_2^+$) [28]. The stability of the three molecular structures is dependent on the pH of the solution with $BTAH_2^+$ stable at pH < 1, BTAH stable at pH values 1 < pH < 8.2, and BTA^- stable at pH > 8.2. The structures of the soluble forms of benzotriazole are shown in Figure 2. The equilibrium reactions between the soluble species are shown below with their equilibrium constants.

$BTAH_2^+ \leftrightarrow BTAH + H^+$ $pk_1 \approx 1$ *Equation 1*

$BTAH \leftrightarrow BTA^- + H^+$ $pk_2 = 8.2$ *Equation 2*

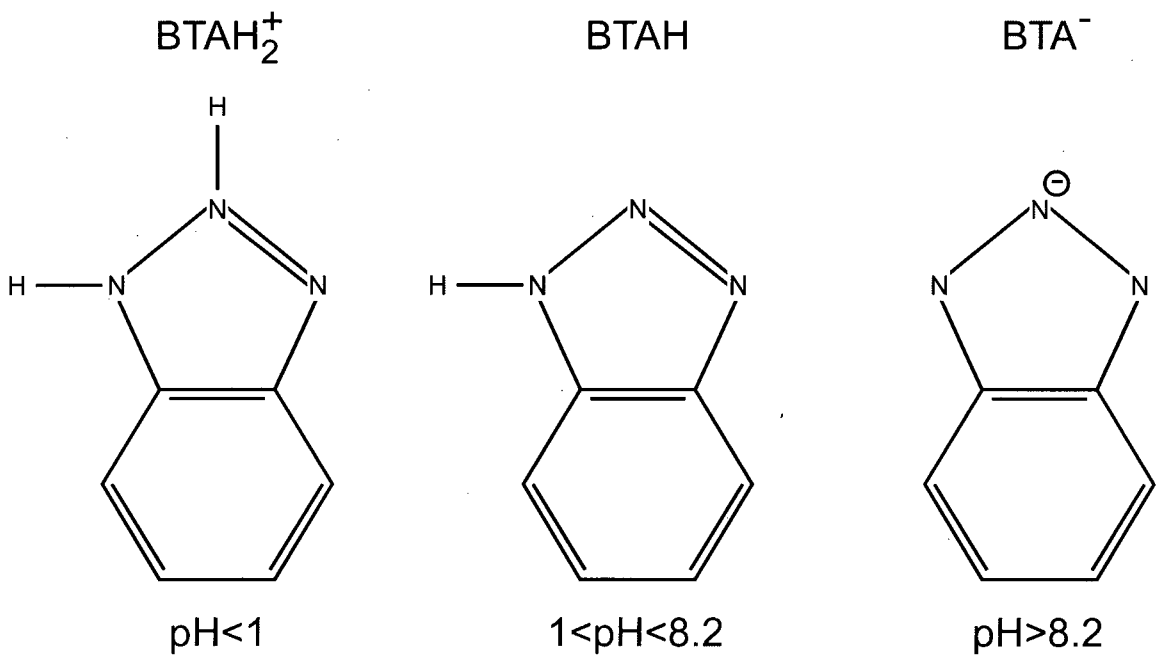

Figure 2 Structures of the soluble forms of benzotriazole

Several studies have concentrated on elucidating the structure of the benzotriazole reaction films. These studies were performed using techniques such as infrared spectroscopy (IRS) [19,20,29,30], electron spectroscopy [20,21,31,32], and Raman spectroscopy [25,33,34,35].

In addition the interaction of copper oxide substrates with solutions containing benzotriazole has been studied using electron spectroscopy [21,36]. Also the structures of adsorbed films produced by vacuum deposition of benzotriazole onto sputter cleaned copper oxide substrates have been studied by IRS [37,38] and ES [38] techniques.

The early studies by Cotton et al. [16,17] postulated that benzotriazole produced a corrosion inhibiting effect by forming a thin (<5 nm) chemisorbed polymeric film of a Cu-benzotriazole complex, shown in Figure 3. Poling [19] confirmed that the complexes contained cuprous species and that the films may reach thickness' up to 500 nm and postulated a polymeric Cu-benzotriazole film with the structure shown in Figure 4. Mansfield & Smith [27] showed that the film thickness can be pH dependent, with thin films being formed in neutral chloride solutions becoming thicker with decreasing pH. Youda et al. [25,35] investigated benzotriazole inhibition in sulphate solutions and determined that complex polymer films are formed at higher electrochemical potentials and pH values, but at lower values benzotriazole molecules are adsorbed.

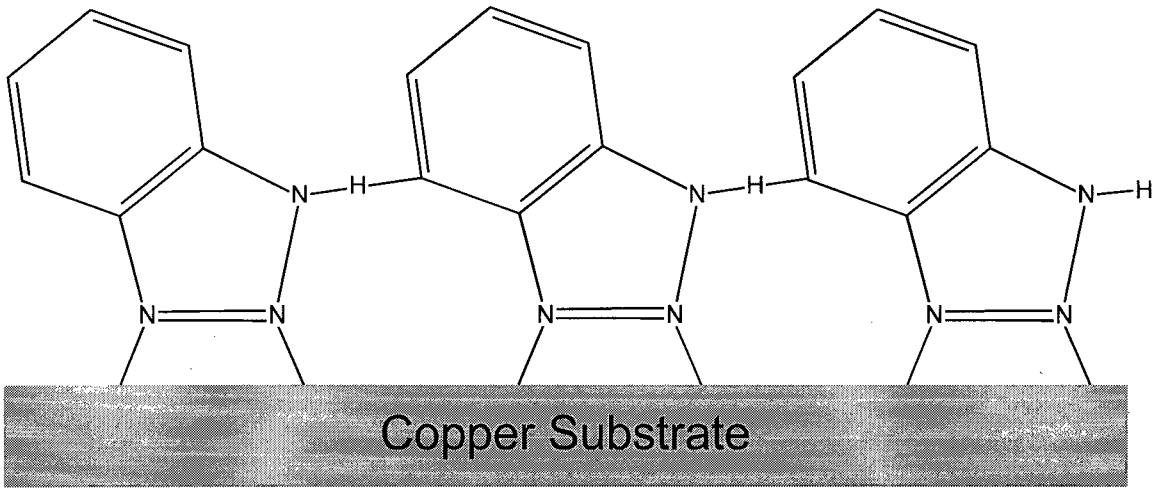

Figure 3 Structure of the chemisorbed monolayer of benzotriazole

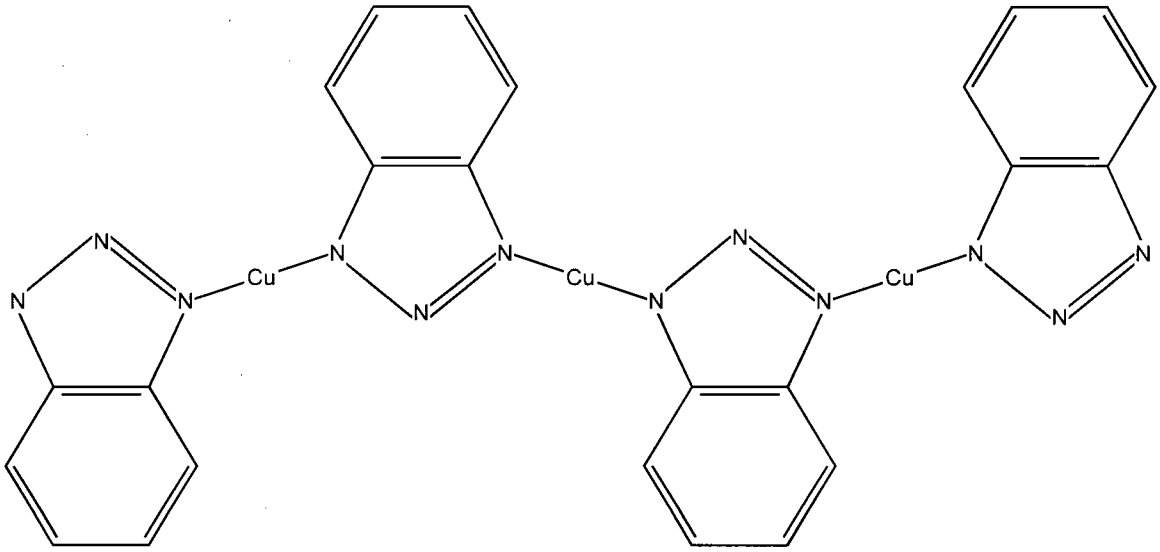

Figure 4 Structure of the copper-benzotriazole polymer complex

Following suggestions that the presence of cuprous oxide (Cu_2O) is necessary for the reaction of benzotriazole with copper [19,27] Ogle & Poling [20] showed that cuprous-benzotriazole polymeric films could be grown on Cu_2O interfaces in chloride solutions. Ogle & Poling also demonstrated that the pH-dependent growth of the polymeric films was linked to the stability of Cu_2O. Several other workers [21,30,31,36] subsequently showed that the Cu_2O interlayer aids the formation of the polymeric films. Hashemi & Hogarth [32] disagreed, believing instead that a cuprous chloride (CuCl) interlayer is necessary. Fang et al. [37] along with Nilsson et al. [38] confirmed that chemisorbtion of benzotriazole can occur on a clean Cu_2O substrates in the absence of an aqueous environment. However, Fang et al. and Nilsson et al. [37,38] also showed that chemisorbtion of benzotriazole can occur on clean copper substrates under the same conditions.

Few studies have been performed studying the interaction of benzotriazole with oxide-free copper surfaces in an aqueous environment [1,31,39]. In principle, creation of an

oxide-free copper surface in an aqueous environment should be possible via cathodic reduction. However, as the interaction between benzotriazole and Cu_2O is reported to be very rapid [31], the cathodic reduction of the oxide layer must be performed prior to the sample being exposed to benzotriazole to ensure that the effect of Cu_2O interlayer is eliminated. The majority of studies investigating the cathodic polarisation behaviour [14,19,20,21,22,23,24,25,33,35] applied cathodic polarisation behaviour only after immersing the copper electrode into a solution containing benzotriazole.

Only Chadwick & Hashemi [31] and Tromans & Sun [1] appear to have added benzotriazole into the environment after the reduction of the copper surface oxide layer. In the study by Chadwick & Hashemi the surface of the copper electrodes were then examined by ES and IRS methods. This examination showed the presence of adsorbed benzotriazole molecules, but failed to reveal the presence of any Cu-benzotriazole complexes. Chadwick & Hashemi concluded that the Cu_2O facilitated the formation of Cu-benzotriazole complexes. However, their investigation did not include any anodic polarisation studies to see whether inhibition was obtained on oxide-free surfaces.

A difficulty involved with anodic polarisation studies of oxide-free copper surfaces is the formation of copper oxides in aqueous solutions at anodic potentials. Tromans & Sun [1] confirmed that in aqueous chloride solutions the formation of $CuCl_2^-$ complexes produced a range of potentials where the anodic dissolution of Cu can occur without the formation of an oxide layer. Following this confirmation, Tromans & Sun performed both potentiostatic and potentiodynamic polarisation studies to elucidate the characteristics of inhibition by benzotriazole. This study confirmed that benzotriazole can interact with oxide-free copper surfaces. This study also showed that the initiation of

inhibition by benzotriazole is both potential and time dependent. As well, a limiting potential was predicted and observed above which benzotriazole additions had no effect and spontaneous repair of existing films no longer occurred.

Tromans & Sun postulated a mechanism of anodic inhibition based on the series of reactions shown below:

$$Cu + BTAH \leftrightarrow (CuBTAH)_{ads}$$ *Equation 3*

$$nCuCl_2^- + nBTAH \leftrightarrow (CuBTA)_n + nH^+$$ *Equation 4*

$$(CuBTAH)_{ads} + (CuBTA)_n \leftrightarrow [(CuBTAH) - (CuBTA)_n]_{ads}$$ *Equation 5*

where the reaction in *Equation 3* is the first limiting step in the formation of the inhibitor film, the adsorption of BTAH onto the Cu electrode surface. The reaction in *Equation 4* is the formation of CuBTA in the diffusion layer. The reaction in *Equation 5* is the formation of a polymeric film as the CuBTA adsorbs onto the $(CuBTAH)_{ads}$ monolayer. The formation of the $(CuBTA)_n$ polymeric film is well established [19] and has been the subject of several studies [17,36,38].

Chapter 2 Objectives

It is has been well defined that benzotriazole (BTAH) forms a corrosion inhibiting diffusion barrier on copper in chloride solutions by adsorbing onto the copper surface and subsequently growing a polymeric film of cuprous-benzotriazole complexes. The objectives of the present study are to:

1. Determine if the similarly structured organic molecules tolyltriazole (TTAH) and methylbenzimidazole (MBM) will exhibit similar characteristics of corrosion inhibition. The molecular structures of BTAH, TTAH and MBM are shown below in Figure 5.

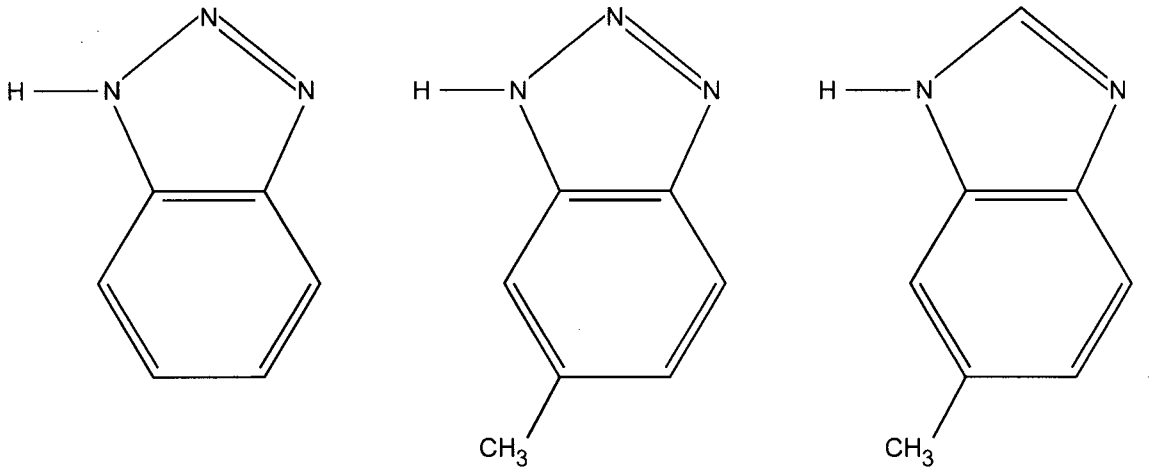

Figure 5 Chemical structure of benzotriazole, tolyltriazole and methylbenzimidazole

Tolyltriazole retains the tri-nitrogen group of the triazole ring intact with the addition of a methyl group attached to the benzene ring. If the site of attachment of the

cuprous ion on the tolyltriazole molecule is other than the tri-nitrogen group, the presence of the methyl group should disrupt the inhibition of anodic corrosion.

The centre nitrogen atom in the triazole ring of methylbenzimidazole is replaced with a carbon atom, disrupting the triazole structure. If the site of the attachment of the cuprous ion is to the triazole ring, methylbenzimidazole should not show inhibiting properties. Methylbenzimidazole also has a methyl group attached to the benzene ring, similar to tolyltriazole.

2. Determine if these molecules provide corrosion inhibition by the same mechanism as benzotriazole.

3. Ascertain whether benzotriazole provided the same corrosion inhibition characteristics in the presence of another halide, bromide.

4. Derive the Potential - pH Diagram for the Cu-Br^--H_2O system to allow analysis of the data obtained in the bromide solutions.

Chapter 3 Experimental

Preparation of the test samples

Cubic working electrodes with 100 mm^2 faces were sectioned from electrical grade copper plate (UNS-C1100) of >99.96% purity by weight. The cubes were annealed at 850 °C for 2.5 hours and cooled. A copper connecting wire was soldered to one face and then, to remove any remaining soldering flux, the cube and wire were washed thoroughly with acetone, etched briefly in HCl, rinsed with distilled water, then methanol and dried with hot blowing air. The wire was sheathed in a glass tube and the assembly was sealed and mounted in epoxy leaving a 100 mm^2 working face exposed. This face was mechanically polished to a 600 grit finish, rinsed with distilled water, then methanol and dried in blowing air. The interface between the copper and epoxy was coated with a cellulose lacquer to prevent any crevice corrosion effects. A schematic of the electrode structure is shown in Figure 6.

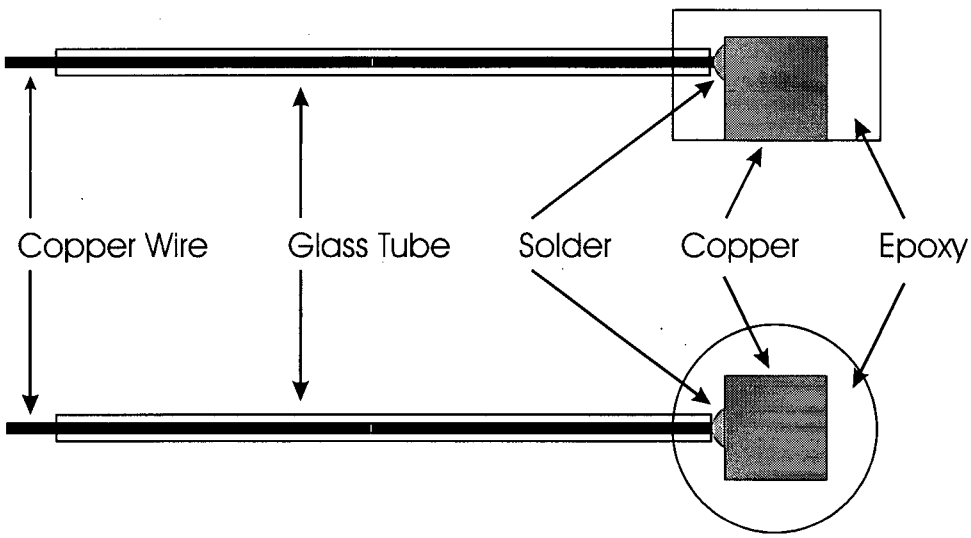

Figure 6 Schematic of the working electrode assembly

It was possible to refurbish and reuse these electrodes by grinding the exposed electrode surface past the depth affected by the last polarisation scan, followed by repolishing using the same procedure described above.

Preparation of the test solutions

1H-benzotriazole, 5methyl-1H-benzotriazole (also known as tolyltriazole), and methylbenzimidazole were obtained from the Aldritch Chemical Company in purities of 99+%, 98%, and 99% respectively. Test solutions either contained no inhibitor, 8.39×10^{-3} M concentration of inhibitor (equivalent to 1 g/l benzotriazole) or 8.39×10^{-4} M concentration of inhibitor (equivalent to 0.1 g/l benzotriazole). Solutions were prepared containing either 1M NaCl, or 1M NaBr. For chloride containing solutions the pH was near neutral (pH 6.54 for solutions without inhibitor and pH 6.0 for solutions with inhibitor) or adjusted with additions of HCl to pH 3.0. For bromide containing solutions the pH was either near neutral (pH 6.54 without inhibitor and pH 6.0 with inhibitor) or adjusted with H_2SO_4 to pH 3.0.

Each solution was prepared by adding the selected inhibitor to a 1 litre volumetric flask with 1 mole of either NaCl or NaBr. The flask was then partially filled with distilled water and a Teflon coated magnetic stir bar added. The flask was then placed on a magnetic stirrer and stirred until all solids were dissolved. The flask was then filled to the 1 litre mark and magnetically stirred. The stir bar was removed and the flask was again filled to the 1 litre mark and agitated by hand for several minutes to ensure proper mixing.

If pH adjustment was required the magnetic stir bar was reinserted and the flask placed on the magnetic stirrer. A combination pH probe was then inserted and the pH monitored as a few drops of 12 M HCl or 12 M H_2SO_4 were added until a pH of 3.0 was achieved. The test solutions used in this study are listed below in Table 1.

Salt Concentration	Inhibitor in Solution	Inhibitor Concentration	Solution pH	pH Adjusted by Addition of
1 M NaCl	None	N/A	Neutral	N/A
1 M NaCl	Benzotriazole	1.000 g/L	Neutral	N/A
1 M NaCl	Benzotriazole	1.000 g/L	3.0	HCl
1 M NaCl	Benzotriazole	0.100 g/L	Neutral	N/A
1 M NaCl	Tolyltriazole	1.114 g/L	Neutral	N/A
1 M NaCl	Tolyltriazole	1.114 g/L	3.0	HCl
1 M NaCl	Tolyltriazole	0.111 g/L	Neutral	N/A
1 M NaCl	Methylbenzimidazole	1.106 g/L	Neutral	N/A
1 M NaBr	None	N/A	Neutral	N/A
1 M NaBr	Benzotriazole	1.000 g/L	Neutral	N/A
1 M NaBr	Benzotriazole	1.000 g/L	3.0	H_2SO_4
1 M NaBr	Tolyltriazole	1.114 g/L	Neutral	N/A
1 M NaBr	Tolyltriazole	1.114 g/L	3.0	H_2SO_4

Table 1 Test solutions

Polarisation test definition

When an electrode is immersed in aqueous solution, electrochemical reactions occur at the electrode/solution interface. The rate and direction of each reaction depends on the potential of the electrode. In order to change the potential from that found under freely corroding conditions it is necessary to apply an external potential to drive the electrode under the desired conditions. In a potentiodynamic polarisation test, the applied potential, which is measured with respect to a standard reference electrode, is continuously varied through the desired range and the corresponding current is recorded.

This recorded current versus applied potential is a polarisation curve. The applied potential in this plot represents the thermodynamic state of the system, and the recorded current represents the sum of all electrochemical reactions occurring at the electrode surface.

Electrochemical cell design

As the corrosion inhibitors studied here have been found to interact strongly with the copper oxide interlayer [31] on the sample electrode surface it was necessary to ensure that the oxide layer was reduced prior to the introduction of the inhibitors into the electrolyte. This procedure ensured that any inhibitor interactions occurred with an oxide free copper surface. It was also necessary to ensure that the dissolved oxygen content of the electrolyte was held at trace levels throughout the test to discourage oxide formation.

To satisfy these conditions, nitrogen gas sparging was used in a two vessel closed atmosphere system. To allow the electrochemical reduction of the oxide interlayer to occur without the inhibitor electrolyte present and to maintain the closed atmosphere, a secondary flask was used to contain half the test electrolyte, which had an inhibitor concentration equal to double that of the desired test concentration. The electrochemical cell contained the remaining half of the test electrolyte, which did not contain any of the inhibitor under study. The secondary flask was connected to the apparatus such that the inhibitor electrolyte from the secondary flask could be added to the electrochemical cell after oxide reduction took place without breaking the closed atmosphere. The apparatus is illustrated in Figure 7.

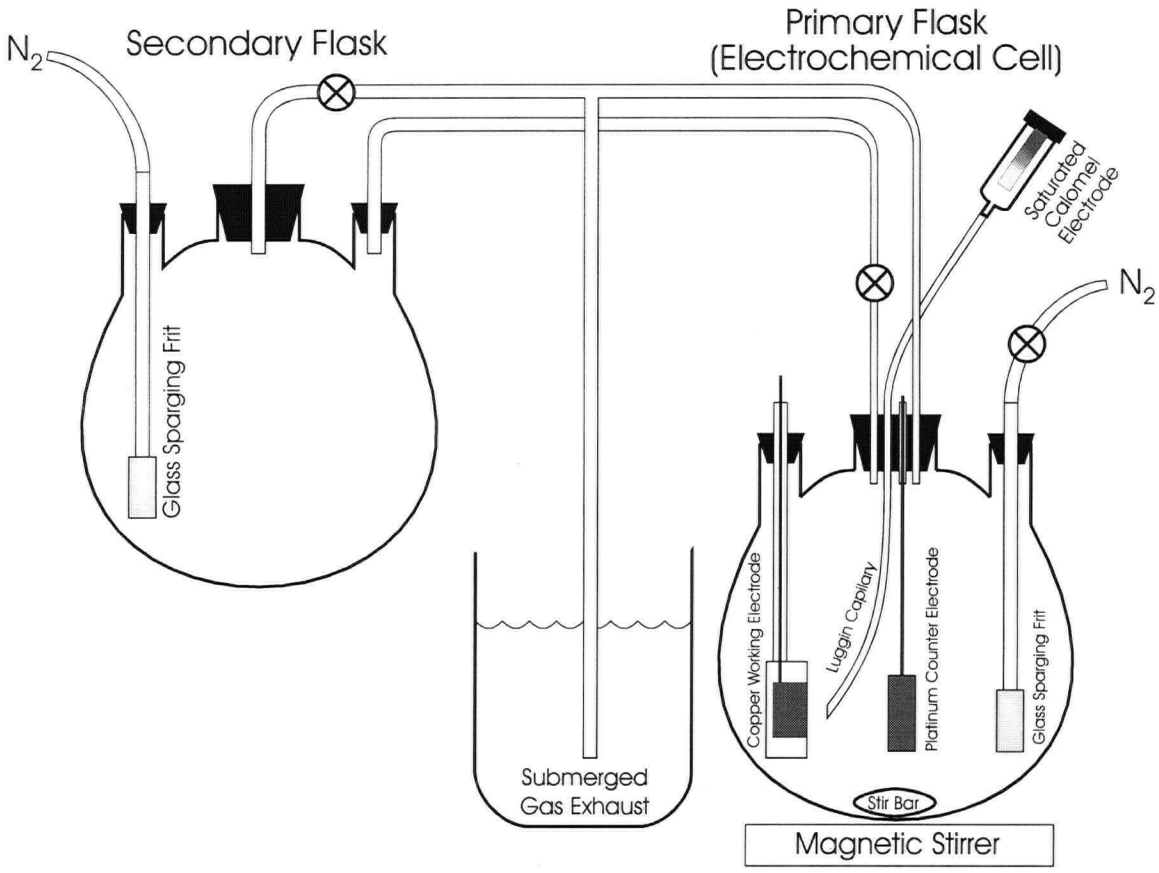

Figure 7 Electrochemical cell apparatus

The electrochemical cell consisted of a three necked glass vessel (except when a scribe was used in which case a four neck vessel was substituted) which contained the sample working electrode, a platinum counter electrode, and a Luggin capillary connecting the reference electrode. The Luggin capillary was filled by drawing solution from the electrochemical cell and connected to an external saturated calomel reference electrode. The tip of the Luggin capillary terminated approximately 0.5 cm from the surface of the sample working electrode. The filling solution was not a significant concern as the electrolyte solutions always contained sufficient ion content from the dissolved salt to be sufficiently conducting. The ohmic (IR) potential drop through the

electrolyte was not corrected for in the test data. The IR drop in the test solutions for several current densities are listed in Table 2. These values were calculated using $\Delta V = (id)/\gamma$ where i is the current density, d is the distance between the tip of the Luggin capillary and the working electrode and γ is the specific conductivity of the electrolyte. For 1M NaCl and 1M NaBr γ = 8.0 and 8.46 $\Omega^{-1}m^{-1}$ respectively [40].

Current Density (A/m^2)		0.1	1	10	100
IR drop (ΔmV)	NaCl	0.062	0.625	6.250	62.500
	NaBr	0.059	0.591	5.910	59.100

Table 2 Values of the ohmic potential drop in solution

The apparatus used to apply the external potential and measure the resulting current was the Parc EG&G model 350 Corrosion Measuring System potentiostat, a microprocessor based system with automated recording of the potential and current measurements. The potentials were measured with respect to a saturated calomel electrode (SCE) connected to the tests electrolyte via a salt bridge containing the working electrolyte. The report potentials can be converted to the standard hydrogen electrode scale via the conversion $V_{SHE} = V_{SCE} + 0.242V$.

The procedure for performing the oxide reduction and subsequent polarisation test began with gas sparging of both flasks with nitrogen to remove any dissolved oxygen in the solutions to trace levels. The gas sparging continued for 20 minutes during which the connecting tube between the two flasks was closed so that the sparging of the flasks remained separate. The exhaust nitrogen from the flasks exited from each flask through tubing to a connecting-T attached to a tube whose end was submerged in a beaker of water to maintain a closed system.

After the 20 minutes concluded the gas sparging continued in the secondary flask, but was discontinued in the primary flask. This was necessary because the presence of gas bubbles in the solution led to blocking of the Luggin capillary and adsorption of bubbles onto the sample electrode surface which disrupted test results and led to premature breakdown or prevented the formation of the inhibitor film in the polarisation test. However, a constantly fed blanket of nitrogen was maintained over the solution in the primary flask during the oxide reduction and polarisation test by opening the connecting tube between the secondary and primary flasks and closing the exhaust connection to the secondary flask. Thus the exhaust nitrogen from the secondary flask (which at this point should be essentially oxygen free) flows into the primary flask providing the blanket of nitrogen over the solution surface. This configuration was maintained throughout the remainder of the test.

After switching the primary flask to a nitrogen blanket the copper sample electrode was then held at -0.900 V_{SCE} for 20 minutes to reduce the surface oxide interlayer. After the 20 minute period of oxide reduction was completed the contents of the secondary flask were added to the primary flask through the connecting tube while maintaining the potential of the sample electrode at -0.900 V_{SCE}. The polarisation scan was then commenced. The potential scan rate was controlled by varying the potential with a staircase waveform produced by the potentiostat. The scan rates were either 1.0 mV/sec or 0.2 mV/sec scanning from -0.900 V_{SCE} to +0.900 V_{SCE}. The data were recorded by the potentiostat and digitally output to a personal computer for graphing and analysis.

Metallographic studies

Polarisation scan samples were prepared for metallographic analysis by following the previously described procedure for performing a polarisation scan at 1.0 mV/s in a solution of neutral pH containing 1.000 g/l BTAH. During these polarisation scans, the upper limiting potential was set to -0.100 V_{SCE}, just above the onset of inhibition observed in earlier polarisation scans. The formation of an inhibition film was confirmed during this procedure by the rapid decrease of the current above -0.250 V_{SCE}. When the sample reached -0.100 V_{SCE}, the sample was maintained at that potential for an additional 15 minutes to provide time for additional thickening of the Cu-BTAH film. The current to the electrochemical cell was then discontinued and the samples were removed from solution, rinsed briefly in distilled water, dried in blowing air, and stored in a desiccator.

Scanning electron microscopy

Changes in surface structure due to the formation of the inhibitor film were studied by scanning electron microscopy (SEM) using 20 kV and 5 kV excitation and secondary electron imaging. The Hitachi Model S-350 SEM system was used.

The initial electron microscopy investigation was performed using a 20 kV excitation that resulted in the surface of the sample rapidly developing a strong surface charge, evident by the sample surface beginning to show as a bright region on the SEM monitor screen. To avoid damage or alterations in the surface structure that might occur due to the surface charging a low excitation of 5 kV was used to prevent the possible vaporisation of the surface inhibitor layer. The 5 kV excitation voltage was used for all further electron microscopy investigations.

Chapter 4 Results

Effect of inhibitor chemical structure on inhibition in chloride solutions

All proposed mechanisms reported in the literature based their models on cuprous complexes forming by copper reacting with the nitrogen atoms of the triazole ring of the inhibitor. In order to confirm that the triazole ring is necessary, two additional compounds with similar chemical structures, tolyltriazole and methylbenzimidazole (Figure 5), were investigated using polarisation scans to determine their effectiveness inhibiting the dissolution of copper.

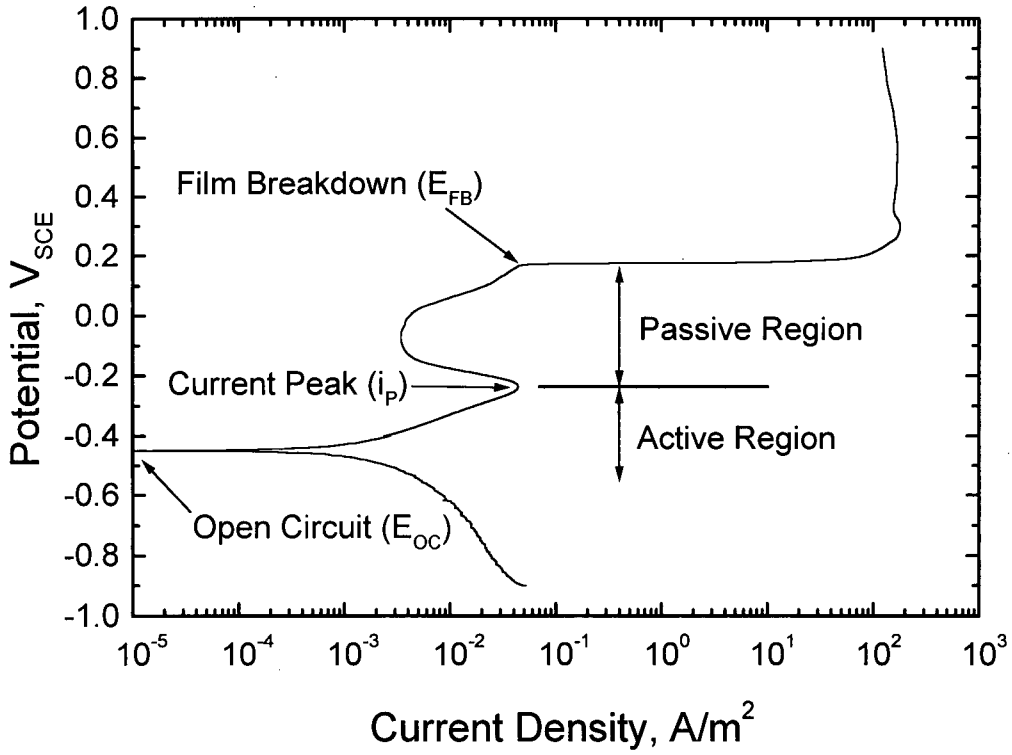

Figure 8 Sample polarisation scan with major features labelled

A sample polarisation scan is shown here in Figure 8 to define the terminology that is used throughout this document.

Polarisation scans were performed with each inhibitor individually in solutions containing 1M NaCl at a scan rate of 1 mV/s, with any oxides present cathodically reduced prior to initiating the scan. These polarisation scans are shown in Figure 9.

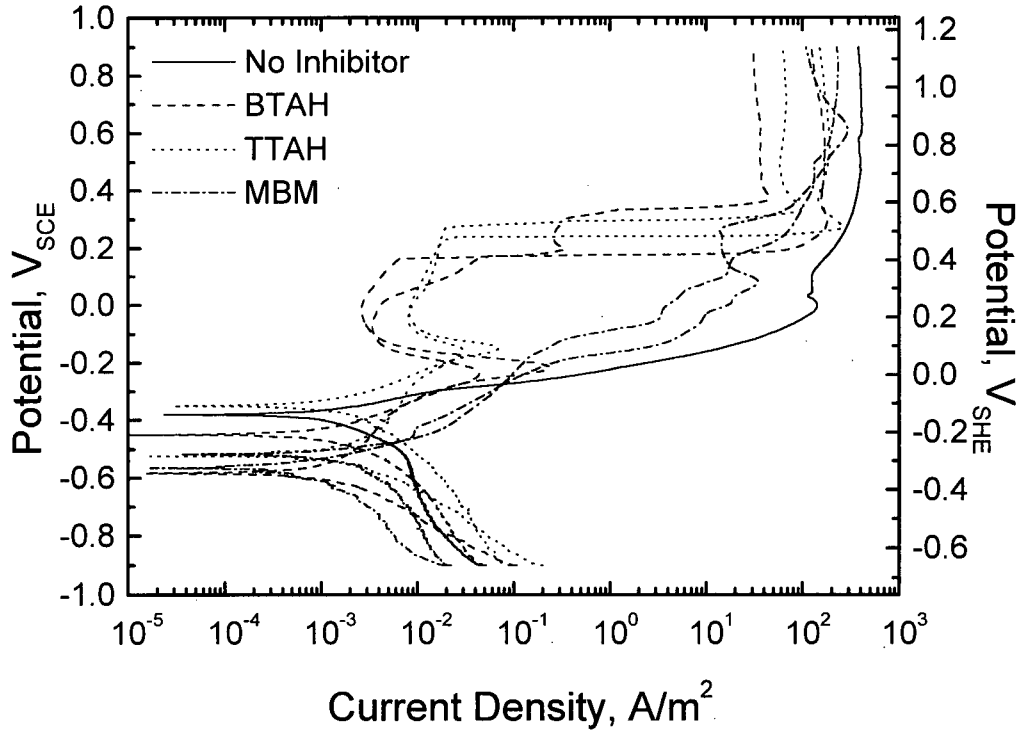

Figure 9 Polarisation scans with no inhibitor, BTAH, TTAH or MBM in 1M NaCl. Scan rate = 1.0 mV/s

The polarisation scans in solutions containing either BTAH or TTAH show well defined current peaks (i_p) at potentials of -0.236 and -0.217 V_{SCE} for benzotriazole and

-0.157 and -0.148 V_{SCE} for tolyltriazole, above which lies a potential region (passive region) where the current density of the anodic reactions is greatly suppressed by up to a factor of 10^4 in comparison with the scan in the solution containing only NaCl, indicating strong inhibition of the anodic dissolution reaction. The polarisation scan performed in solutions containing MBM did not contain any current peaks that indicating the onset of an inhibition reaction caused by the formation of a polymeric film. In general the behaviour of copper in solutions containing MBM showed inhibition above -0.2 V_{SCE} reducing the current density by up to a factor of 100 with no well-defined current peak.

The position of the open circuit potential (E_{OC}) varied considerably, spanning a range of potentials from -0.350 to -0.600 V_{SCE}. In the study by Tromans and Sun [1] the E_{OC} presented the same behaviour and it was shown that the position of E_{OC} was primarily controlled by the reduction of traces of dissolved oxygen in solution. Thus the variation of the position of E_{OC} is an indication of the variation in the concentration of the dissolved oxygen between different polarisation scans. The positions of the open circuit potential (E_{OC}) was generally lower in solutions containing the organic molecules than in solutions containing NaCl only. This indicates that the organic molecules were weakly adsorbing on the sample surface providing a weak inhibition of the cathodic reactions.

The potential at i_p is ~70 mV higher in solutions containing TTAH than for solutions containing BTAH. The same is true of the potential where the onset of inhibition film breakdown first occurs (E_{FB}). The size of the range over which the inhibition of the anodic dissolution reaction occurs is approximately the same for BTAH as TTAH. However, the polarisation scans performed in solutions containing BTAH displayed a greater reduction in the current density of the anodic dissolution reaction than exhibited in the solutions containing TTAH.

Effect of scan rate on benzotriazole and tolyltriazole inhibition

Polarisation scans were performed in 1 M NaCl solutions containing either 1.000 g/L BTAH or 1.114 g/L TTAH (molar equivalent to 1 g/L BTAH). The polarisation scans were performed at scan rates of 1.0 mV/s and 0.2 mV/s to determine which characteristics of inhibition behaviour are thermodynamically controlled and which are controlled by kinetic effects. The polarisation scans performed in solutions containing 1.000 g/L BTAH are shown in Figure 10. The polarisation scans performed in solutions containing 1.114 g/L TTAH are shown in Figure 11.

In Figure 10 the potentials at which i_p occurs are at values of -0.236 and -0.217 V_{SCE} for a scan rate of 1 mV/s and at -0.283 and -0.239 V_{SCE} for a scan rate of 0.2 mV/s, showing that the potential at which i_p occurs is ~34 mV more negative at the slower scan rate. The maximum current density reached at i_p is dependent on the scan rate, reaching an average maximum current density of 0.1389 A/m^2 during experiments performed at a scan rate of 1.0 mV/s and reaching an average maximum current density of 0.0253 A/m^2 during experiments performed at a scan rate of 0.2 mV/s.

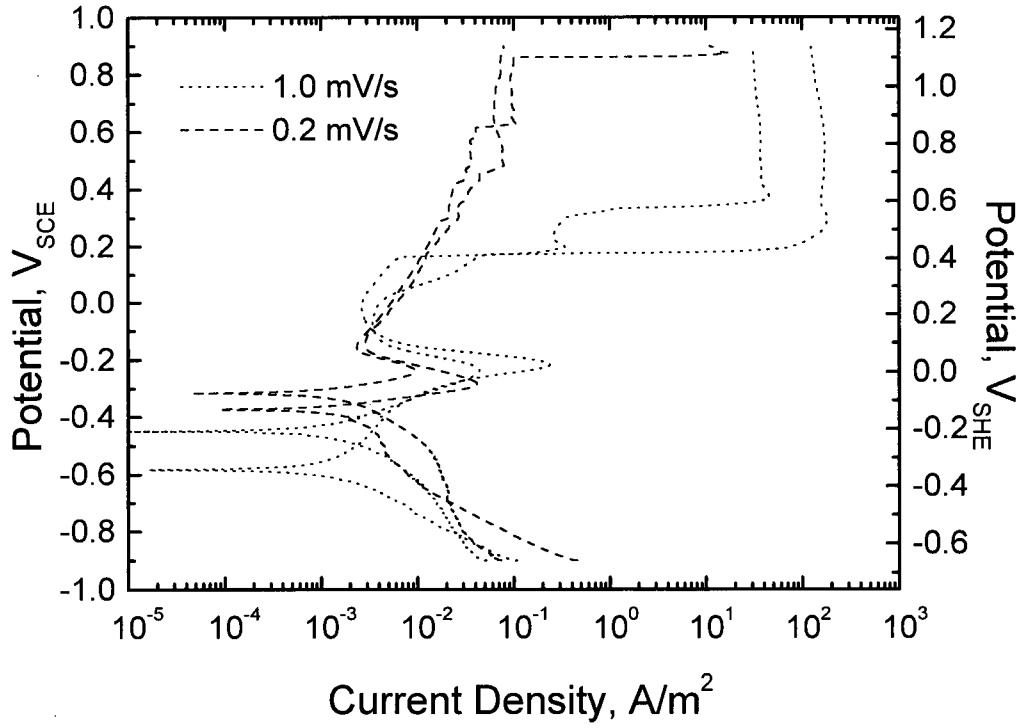

Figure 10 Polarisation scans in 1M NaCl containing 1.000 g/l BTAH

The potential at which the breakdown of the inhibition film occurred (E_{FB}) was affected by changes in scan rate with a scan rate of 0.2 mV/s delaying the breakdown of the inhibition film until potentials near +0.900 V_{SCE} whereas the breakdown of the inhibition film occurred at a potential of 0.167 V_{SCE} when employing a scan rate of 1.0 mV/s. In some scans performed at 0.2 mV/s the inhibition films did not breakdown within the potential range of the experiment, continuing to greatly decrease the rate of anodic dissolution of copper above the onset of inhibition potential. E_{FB} did not always result in complete breakdown of the inhibition film, with some polarisation scans producing only partial increases in current density indicating that a localised breakdown

had occurred. During these scans, film breakdown was evidenced by the appearance of dark green spots of corrosion product appearing at the sites of the breakdown, with the reminder of the sample surface remaining bright. At a higher potential where full breakdown occurred, the entire sample surface would become covered with the corrosion products. An example of this behaviour is shown in Figure 10 during one of the scans performed at 1.0 mV/s, where the initial localised breakdown of the inhibition film occurred at 0.167 V_{SCE} and the complete breakdown occurred at 0.335 V_{SCE}.

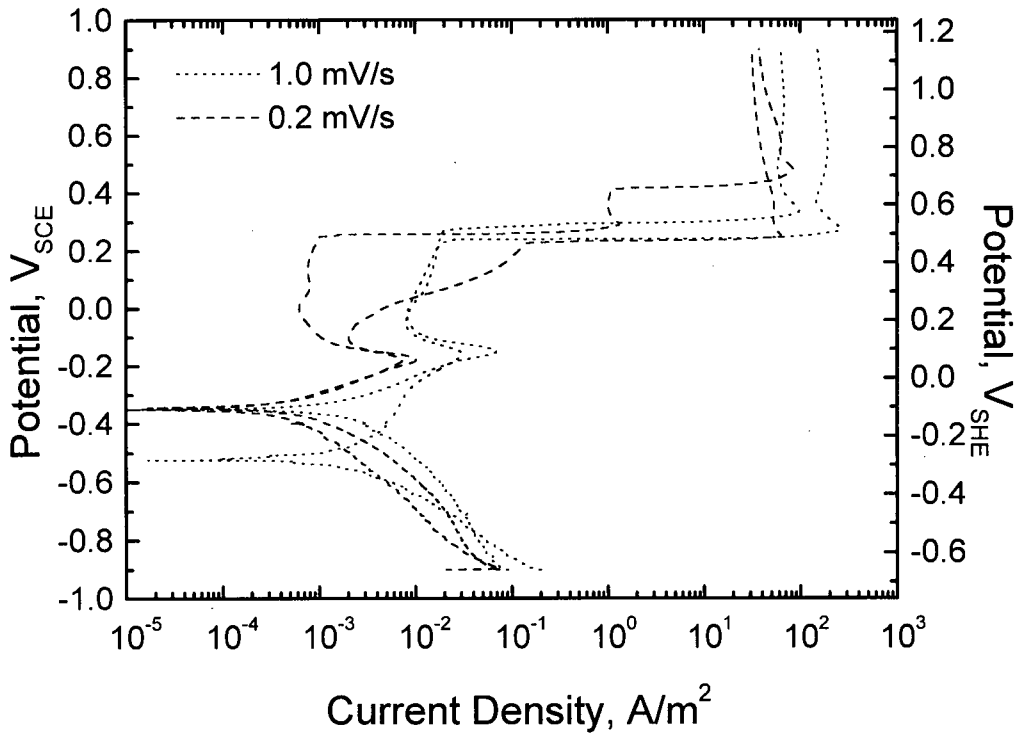

Figure 11 Polarisation scans in 1M NaCl containing 1.114 g/l TTAH

In the results of polarisation scans in solutions containing 1.114 g/L TTAH shown in Figure 11, i_p occurred at potentials of -0.157 and -0.148 V_{SCE} at a 1.0 mV/s scan rate,

and at -0.178 V_{SCE} at 0.2 mV/s scan rate, showing the onset of inhibition occurred ~26 mV more negative at the slower scan rate, similar to the behaviour observed in the solutions containing BTAH described earlier. The maximum current density reached at this peak was affected by changes in the scan rate with an average maximum current density of 0.0496 A/m^2 being reached in experiments performed at 1.0 mV/s and an average maximum current density of 0.0087 A/m^2 in experiments performed at 0.2 mV/s.

In the solutions containing TTAH however, a lower scan rate did not result in an increase in the potential at which inhibition film breakdown would occur. The breakdown of the inhibition film formed by TTAH occurred at 0.242 and 0.271 V_{SCE} for scans performed at 1.0 mV/s, and at 0.227 and 0.258 V_{SCE} for scans performed at 0.2 mV/s. As with the scans performed in solutions containing BTAH, an initial localised breakdown would sometimes occur prior to a complete breakdown. This was evidenced by a sudden partial increase of current density followed by a current plateau. During the same time period local spots of dark green corrosion product would appear on the sample surface while the remainder of the sample would remain bright and unchanged. At a higher potential the current density would make another abrupt increase at the same time that the sample surface would become completely covered in corrosion product, indicating a full breakdown of the inhibiting film. This is displayed in Figure 11 during one of the scans performed at 0.2 mV/s, where the initial localised breakdown occurred at 0.258 V_{SCE} and the final breakdown was delayed until 0.414 V_{SCE}.

Effect of inhibitor concentration on benzotriazole and tolyltriazole inhibition

Polarisation scans were performed at a scan rate of 1.0 mV/s in solutions containing BTAH concentrations of 1.0 and 0.1 g/L and in solution containing TTAH concentrations of 1.114 or 0.111 g/L to determine which inhibition aspects were dependent on the kinetics of the system. The results are shown in Figure 12 for the solutions containing BTAH and in Figure 13 for solutions containing TTAH.

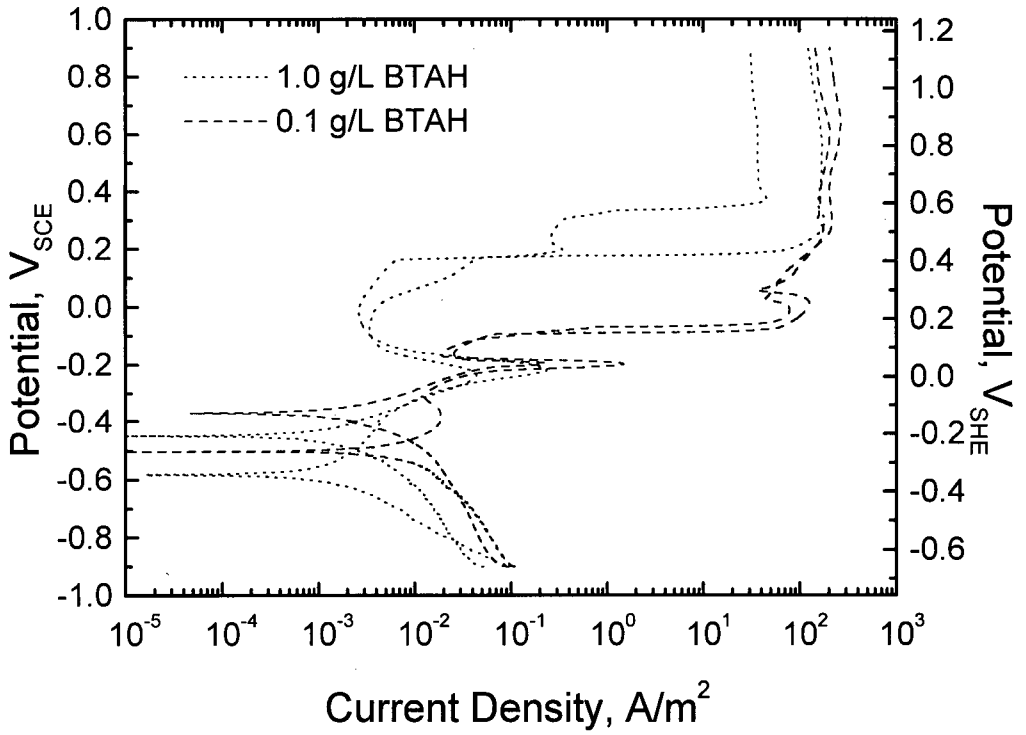

Figure 12 Polarisation scans in 1M NaCl containing 1.000 or 0.100 g/l BTAH. Scan rate = 1.0 mV/s

The open circuit potential E_{OC} in Figure 12 does not appear to be affected by changes in BTAH concentration and varied between -0.600 V_{SCE} and -0.375 V_{SCE}. The

potential at which the current peak (i_p) occurred increased slightly from -0.226 V_{SCE} to -0.197 V_{SCE} with a decrease in BTAH concentration from 1.0 g/L to 0.1 g/L. The maximum current density reached at this current peak was affected by the inhibitor concentration with an average maximum current density of 0.8471 A/m^2 in experiments performed with 0.2 g/L BTAH concentration, and an average maximum current density of 0.1389 A/m^2 in experiments performed with 1.0 g/L BTAH. However, the average potential at which the breakdown of the inhibition film initially occurred decreased from 0.167 V_{SCE} to -0.082 V_{SCE} with a decrease in BTAH concentration from 1.0 to 0.1 g/L reducing the range of potentials within which the corrosion inhibition is effective.

The E_{OC} in solutions containing TTAH (Figure 13) does not appear to change with changing TTAH concentrations, varying between -0.525 V_{SCE} and -0.350 V_{SCE}. Inhibition of the anodic dissolution reaction did not occur consistently between experimental runs of solutions containing 0.111 g/L TTAH, with inhibition occurring during some experiments, and a complete lack of inhibition occurring during others.

In polarisation scans performed in solutions containing 0.111 g/L TTAH where inhibition occurred, the onset of inhibition was represented by a short, blunt current peak deviating from the apparent Tafel slope of the anodic dissolution reaction occurring at -0.218 V_{SCE}. The current density did not decrease significantly above the current peak, remaining at a rough plateau of approximately 0.05 A/m^2 until compete breakdown of the inhibiting film occurred.

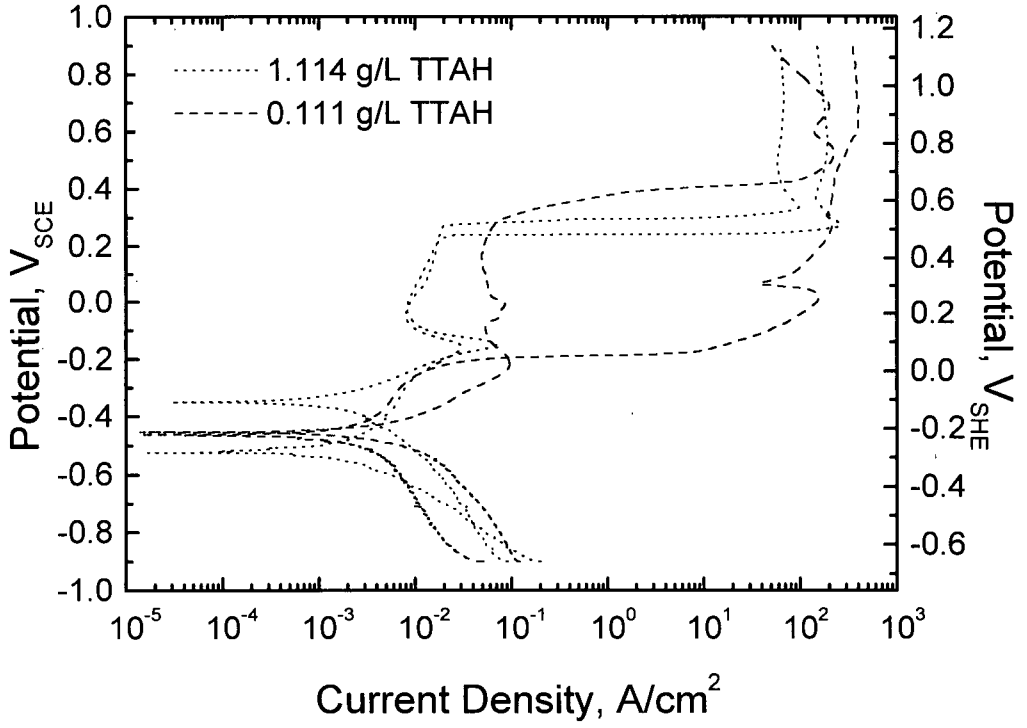

Figure 13 Polarisation scans in 1M NaCl containing 1.114 or 0.111 g/l TTAH. Scan rate = 1.0 mV/s

In solutions containing TTAH, E_{FB} occurred at 0.232 and 0.271 V_{SCE} for 1.114 g/L TTAH and in the vicinity of 0.280 V_{SCE} for 0.111 g/L TTAH showing that the breakdown potential did not appear to be affected significantly by changes in the concentration of the inhibitor.

The Cu-Br^--H_2O system potential-pH equilibria

Since the present study involves investigations of the behaviour of copper in aqueous bromide solutions, the thermodynamically stable species need to be identified to be able to properly analyse the experimental data.

The Pourbaix diagram is a thermodynamic diagram of aqueous chemical equilibria where the predominant dissolved and solid species are represented on a plot in a standard format of potential versus pH. This form of diagram is commonly used in studies of metal corrosion. The Pourbaix diagram for the Cu-H_2O system is widely known [41]. Several studies have been published on the Pourbaix diagram for the Cu-Cl^--H_2O system [10,39,42,43,44,45,46]. However, the Pourbaix diagram for the Cu-Br^--H_2O system could not be found in the literature.

Established procedures [39,41] were used to calculate the chemical and electrochemical equilibria from free energy data for the Cu-Br^--H_2O system. The standard chemical free energies of all species considered are listed in Table 3 together with the sources for the data. Free energy data for the $CuBr_2^-$ species was found only in the older literature [11,12] and is probably the least precise. It should, however, be sufficiently accurate for the purposes of the present study. The remaining data were obtained from more recent sources [10,47] and are close to the values compiled by Wagman et al. [9].

The resulting potential-pH equilibria diagram for the Cu-Br^--H_2O system at 25 °C is presented in Figure 14. Solid lines on the diagram outline the stability regions of solid phases in equilibrium with 10^{-8}, 10^{-6}, 10^{-4}, and 10^{-2} activities of soluble copper species. Fine broken lines show the equilibria between dissolved species. The coarse broken lines, labelled "a" and "b", are the pH-dependent standard hydrogen electrode and oxygen electrode potentials, respectively, at unit gas fugacity. Figure 14 is constructed with respect to a [Br^-] activity of 0.7, corresponding to a 1M NaBr solution. The activity was calculated by converting the molarity (1M) to molality (1.02 m) and using the

molality dependent activity coefficient of 0.687 that is reported in the Handbook of Chemistry and Physics [48].

Species	State	G°, (kJ/mole)	Ref.
H^+	aq	0	47
H_2	g	0	47
O_2	g	0	47
H_2O	l	-237.178	47
OH^-	aq	-157.293	47
Cu	s	0	10
Cu^+	aq	+50.3	10
Cu_2^+	aq	+65.7	10
$HCuO_2^-$	aq	-258.9	10
CuO_2^{2-}	aq	-183.9	10
Cu_2O	s	-148.1	10
CuO	s	-134	10
Br^-	aq	-103.97	47
$CuBr_2^-$	aq	-189.12	11,12
CuBr	s	-101	47
$CuBr_2$	s	-123	47

Table 3 Standard chemical free energies (G°) at 25°C

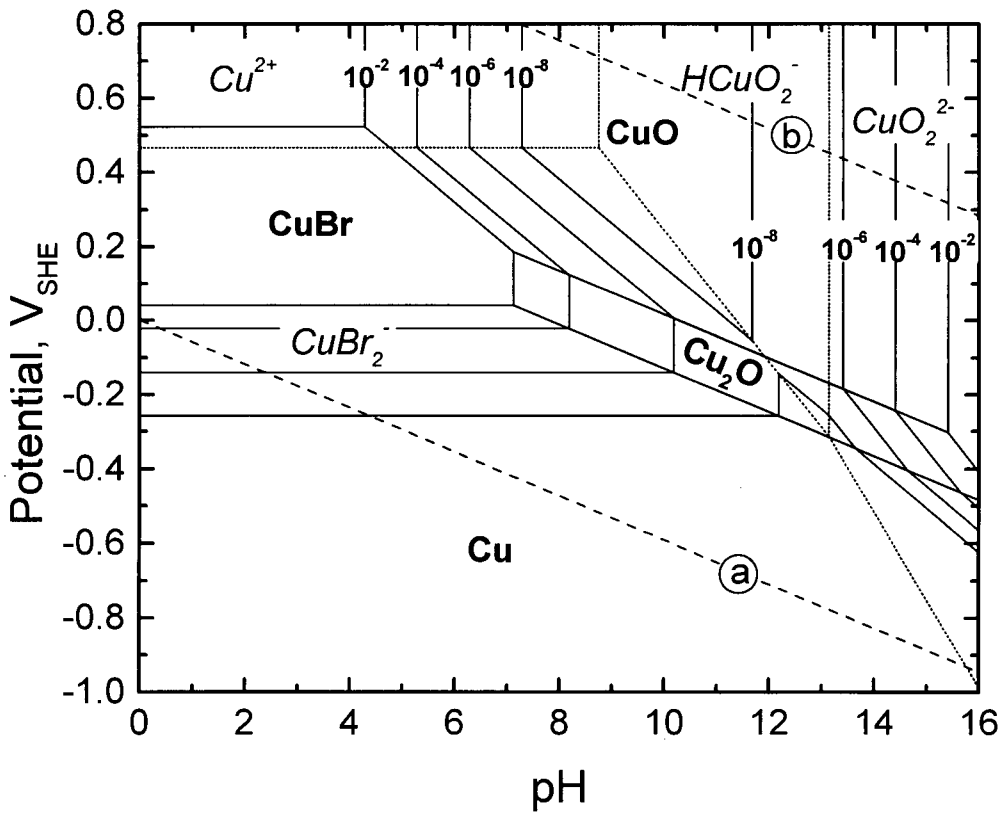

Figure 14 Potential-pH equilibria for the Cu-Br^--H_2O system

Comparing Figure 14 with the simple Cu-H_2O system in Figure 15 [1] shows that the formation of $CuBr_2^-$ complexes extends the copper solubility range to both lower potentials and higher pH values by destabilising the formation of copper oxides and promoting more active behaviour of the metal. The overall effects of the addition of bromide ions on the stability of cuprous complexes, as well as the overall appearance of the diagram, are closely similar to those of chlorides, shown in Figure 16 [1].

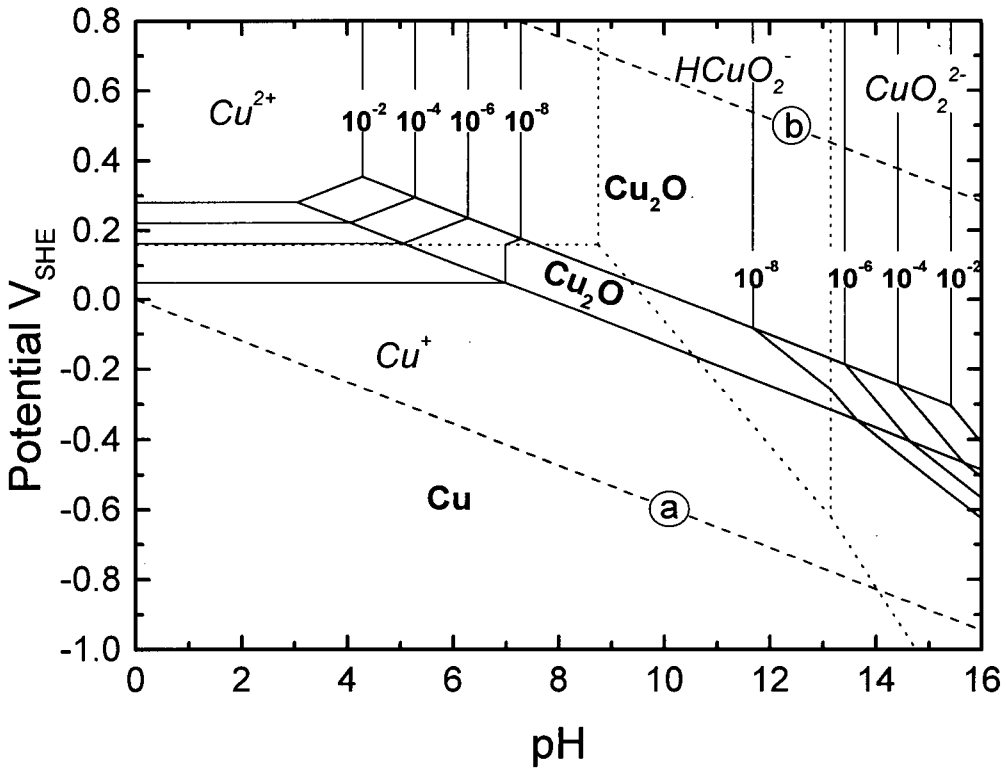

Figure 15 Potential-pH equilibria for the Cu-H_2O system

In Figure 16 the area labelled with "*" indicates the region where $CuCl_2 3Cu(OH)_2$ is the stable specie.

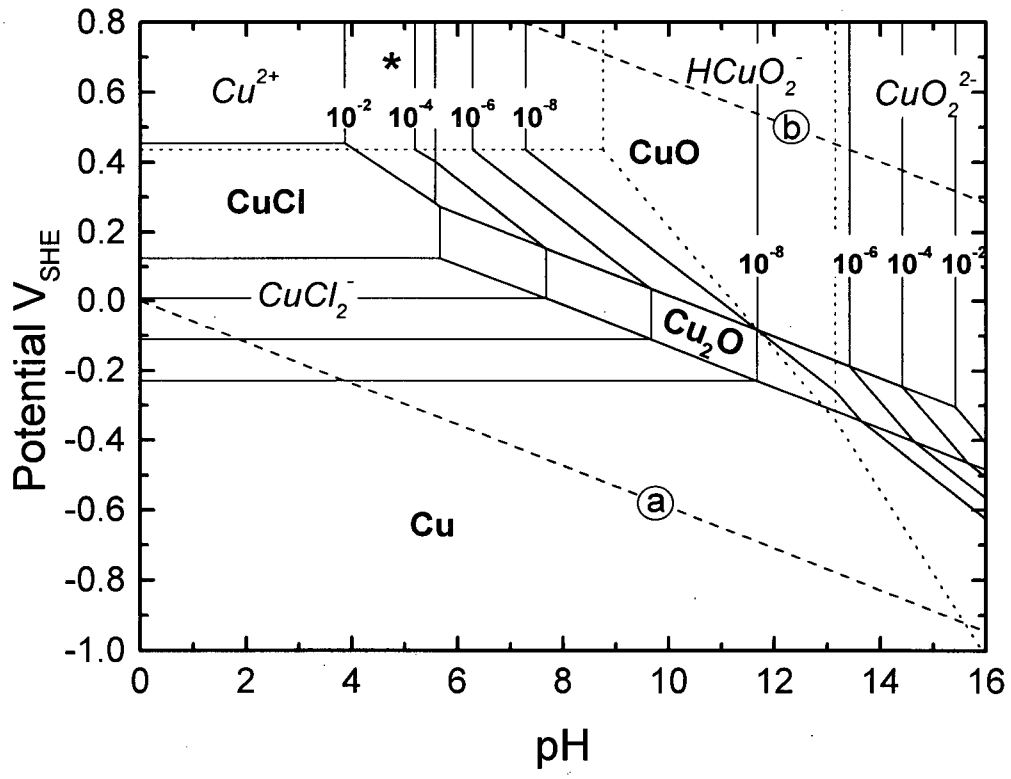

Figure 16 Potential-pH equilibria for the Cu-Cl⁻-H_2O system

Equation 6 and *Equation 8* below show the equilibria between copper and bromous species in the presence of and absence of bromide respectively. *Equation 7* and *Equation 9* are the corresponding Nernst equations at 25 °C.

$$CuBr_2^- + e^- \leftrightarrow Cu + 2Br^- \qquad \textit{Equation 6}$$

$$E_{CuBr_2^-/Cu} = +0.195 + 0.059 \log\left(\frac{[CuBr_2^-]}{[Br^-]^2}\right), V_{SHE} \qquad \textit{Equation 7}$$

$$Cu^+ + e^- \leftrightarrow Cu \qquad \textit{Equation 8}$$

$$E_{Cu^+/Cu} = +0.52 + 0.059 \log[Cu^+] \text{, } V_{SHE} \qquad \textit{Equation 9}$$

The equilibrium reaction between Cu and CuBr is shown in *Equation 10*. The corresponding Nernst potential at 25 °C is presented in *Equation 11*.

$$CuBr + e^- \leftrightarrow Cu + Br^- \qquad \textit{Equation 10}$$

$$E_{CuBr/Cu} = +0.031 - 0.059 \log[Br^-] \text{, } V_{SHE} \qquad \textit{Equation 11}$$

Hence CuBr forms at +0.040 V_{SHE} and appears in Figure 14. At this potential the equilibrium activity of $[CuBr_2^-]$ is 1.16×10^{-3}.

The calculations of thermodynamic equilibria based on a $[Br^-]$ activity of 0.7 suggest two important effects on the aqueous corrosion behaviour of copper relative to the Cu-H_2O system. First, the presence of bromide ions in solution allows corrosion (dissolution) to occur over a range of potentials in near neutral solutions without the formation of copper oxides. Second, in acidic and near neutral solutions, anodic dissolution of the metal will be depressed to more active potentials and should be governed by the formation of soluble copper species in the Cu^I (cuprous) state. These effects are similar to those produced by Cl^- additions (Figure 16) [1].

Polarisation behaviour of copper in bromide solutions

Thermodynamic predictions relating to the behaviour of copper in bromide solutions were tested by conducting polarisation scans on copper in bromide solutions in near neutral (pH 6.5) and acidic solutions (pH 3.0) of 1 M NaBr. The resulting polarisation behaviours are shown in Figure 17.

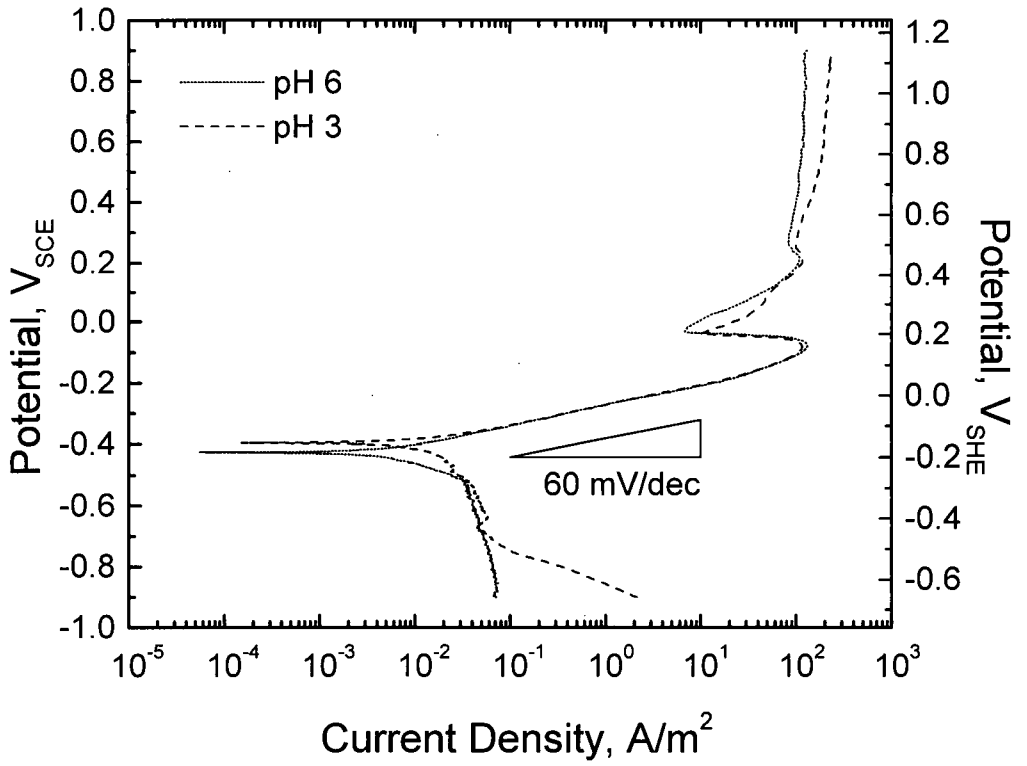

Figure 17 Polarisation behaviour of Cu in 1M NaBr at pH 6.5 and 3.0. Triangular insert shows a slope of 60 mV per decade in current density

The behaviour in both solutions was very similar and independent of pH. The open circuit potentials (E_{OC}) are close to -0.400 V_{SCE} (approximately -0.150 V_{SHE}) and are approximately 200 mV more active than those observed in sulphate solutions where copper does not form soluble complexes [1]. Above E_{OC}, there is a region of active dissolution of copper with an apparent Tafel slope ($d E / d \log i$) of 60 mV per decade of current density, very similar to that observed previously in chloride solutions [1,3,4,5,6], as in the inhibitor free test shown in Figure 9. Comparison of the range of potentials where active behaviour occurs with the aqueous equilibria in Figure 14 shows that the active

region is consistent with the dissolution reaction being the formation of soluble $CuBr_2^-$ complexes.

The apparent Tafel region departs from linearity at a potential of -0.180 V_{SCE}. This is a result of the ohmic potential drop (ΔV) due to the electrical resistance of the solution and formation of solid CuBr. A major current peak of ~130 A/m^2 is observed close to -0.080 V_{SCE}. After correcting for a ΔV of 82 mV, the true peak potential is calculated to be -0.162 V_{SCE} (+0.080 V_{SHE}). This value corresponds very closely to the equilibrium potential for the formation of CuBr at +0.040 V_{SHE}, as calculated using *Equation 10* and *Equation 11*. Therefore this current peak is associated with the film formation arising from the lateral growth and film thickening of CuBr nuclei that begin forming at +0.040 V_{SHE}, causing any further oxidation to occur under the mass transport controlled kinetics limited by the movement of ions through the film. The current plateau occurring at higher potentials can then be attributed to the presence of a weakly passivating CuBr salt film. This is consistent with the observation that a loosely adhering corrosion product with a greenish coloration began to appear at this potential [49].

A small secondary anodic current peak is present near +0.204 V_{SCE} that is probably caused by the oxidation of Cu^I to Cu^{II}. The ΔV corrected potential corresponds to +0.144 V_{SCE} (+0.386 V_{SHE}). As the potential of this current peak was pH independent, it suggests that the peak corresponds to the oxidation of the cuprous bromide complex ($CuBr_2^-$) to Cu^{2+}, via *Equation 12* at potential given by *Equation 13*.

$$CuBr_2^- \leftrightarrow Cu^{2+} + 2Br^- + e^- \qquad \textit{Equation 12}$$

$$E_{Cu^{2+}/CuBr_2^-} = +0.48 + 0.059 \log\left(\frac{[Cu^{2+}][Br^-]^2}{[CuBr_2^-]}\right), V_{SHE} \qquad \textit{Equation 13}$$

Equation 12 shows that Cu^{2+} is the dominant soluble copper species above +0.467 V_{SHE} when the [Br-] activity is 0.7. This indicates that oxidation of $CuBr_2^-$ to Cu^{2+} should occur near this potential, consistent with the position of the secondary peak.

In summary, there was a good overall correlation between the anodic polarisation characteristics of copper in aqueous bromide solutions (Figure 17) and the predictions of anodic behaviour based on the thermodynamic equilibria (Figure 14). The most important point is that a significant region of active behaviour is predicted and observed that is related to the formation of cuprous bromide complexes, analogous to the formation of Cu^I complexes in chloride solutions [1].

Polarisation behaviour of copper in bromide solutions containing benzotriazole

The presence of BTAH tended to have little effect on either the E_{OC} potential or the initial anodic behaviour near E_{OC}, irrespective of the pH. However, significant current deviations commenced at slightly higher potentials in the active region. For the BTAH containing solutions, the current deviations occurred between -0.310 to -0.250 V_{SCE} in the pH 6.0 solutions and between -0.260 to -0.250 V_{SCE} in the pH 3.0 solutions. These deviations resulted in large decreases in anodic current density relative to the inhibitor free solution. This indicates that anodic inhibition had occurred on oxide-free surfaces and that this inhibition was not effective until potentials between approximately -0.300 V_{SCE} and -0.250 V_{SCE} (approximately -0.060 to 0.010 V_{SHE}) were reached. The

characteristic features of the polarisation curves are shown in Figure 18 and Figure 19, at pH values of 6.0 and 3.0 respectively. Two curves for each pH and each inhibitor are presented to demonstrate the degree of reproducibility, and both figures contain the corresponding polarisation curve for the inhibitor free solution for comparison purposes.

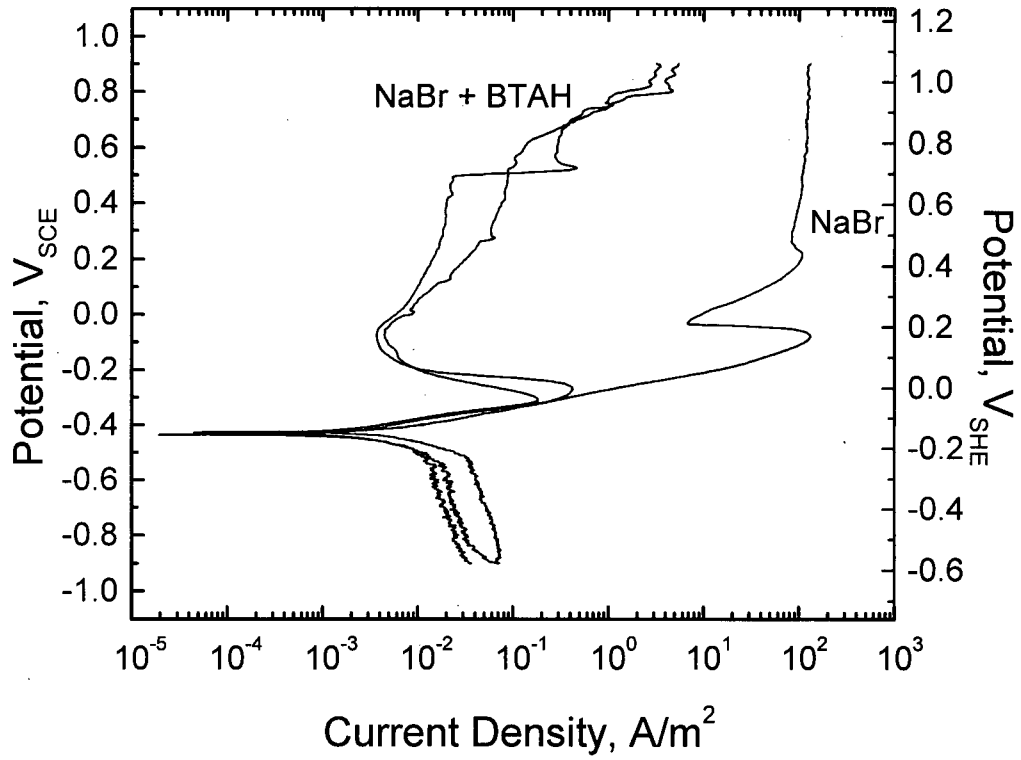

Figure 18 Polarisation behaviour of Cu in 1M NaBr containing 1.0 g/l BTAH at pH 6.0. Behaviour compared with as prepared 1M NaBr (pH 6.5)

Figure 18, at pH 6.0, clearly shows that the onset of inhibition near -0.250 V_{SCE} produces a current peak and a rapidly decreasing current density followed by a very low current density plateau that is typically indicative of the formation of a passive film. Passive currents in BTAH containing solutions as low as 3.7×10^{-3} A/m^2 were obtained

near -0.072 V_{SCE}, and these current densities remained relatively low as the potential was scanned to near +0.5 V_{SCE}. There was a gradual increase in current at more noble potentials, indicating changes in the passive film, but the current density remained lower than in the inhibitor-free solution.

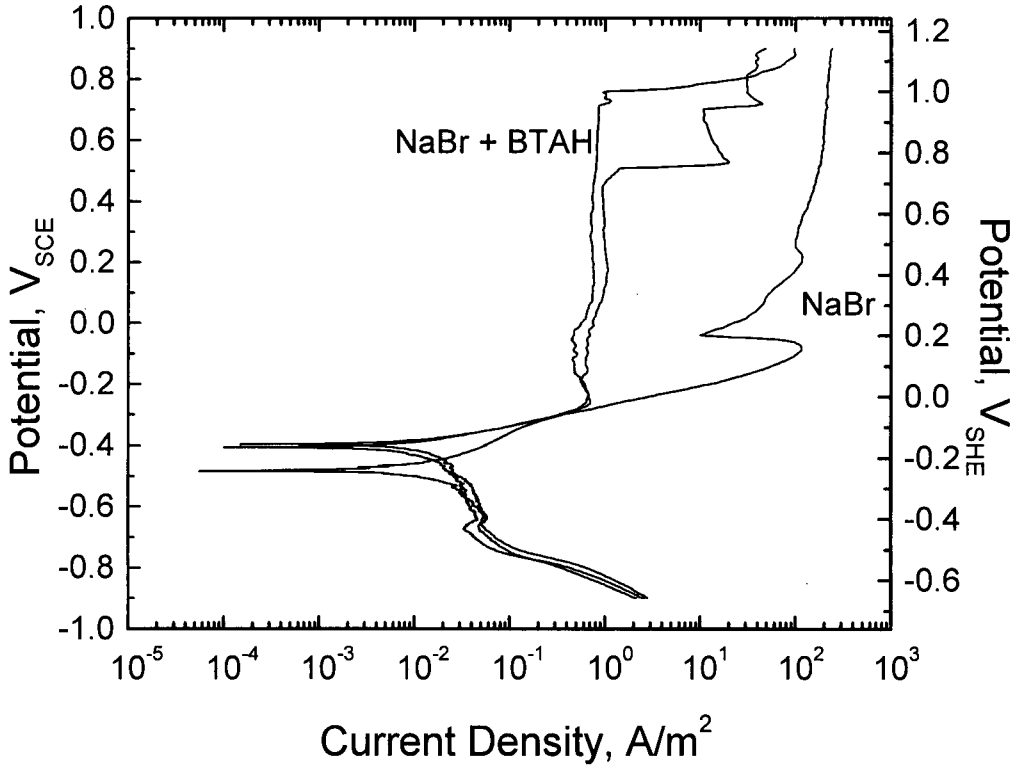

Figure 19 Polarisation behaviour of Cu in 1M NaBr containing 1.0 g/l BTAH at pH 3.0 Behaviour compared with 1M NaBr at pH 3.0

Similar to the behaviour at pH 6.0, an active-passive transition occurs in the pH 3.0 solution, as shown in Figure 19, but the passive current densities in the plateau region are significantly higher (approximately 1 A/m^2) than at pH 6.0. These differences suggest that the structure of the passive film is pH dependent, resulting in less anodic

inhibition as the pH decreases. This behaviour is analogous to that observed in chloride solutions containing BTAH [1].

Stability and breakdown of inhibitor films

Breakdown of Cu-BTAH complex passive films occurred at higher potentials. It was signalled by a pronounced increase in current density and was accompanied by the formation of pits on the copper electrode surface containing a green corrosion product in the form of a tubercule, consistent with the appearance of CuBr. However, the stability region of the inhibiting passive film was not found to be reproducible. For example, in the pairs of duplicate tests in Figure 18, and Figure 19, a pronounced current density increase occurred near +0.5 V_{SCE} in one test and was delayed until much higher potentials in the other test. Also, very small transient current peaks were observed in the passive region suggesting a film breakdown and repassivation phenomenon. These small peaks are most clearly shown in Figure 18, and to a lesser extent in Figure 19.

Therefore, to determine whether a mechanically damaged film could undergo spontaneous repassivation or repair in the passive region, a diamond scribe was used to scratch the surface of a copper electrode during a polarisation test at pH 6.0. The results are shown in Figure 20. In this test the inhibition and film formation were allowed to occur prior to scratching the electrode surface. The anodic current peak close to -0.295 V_{SCE} and subsequent current decrease confirm that inhibition occurred. After inhibition and film formation occurred the surface was rapidly scribed at -0.150 V_{SCE}. Comparison of Figure 20 with Figure 18 shows that after scribing the current density increased 100 times relative to the unscribed surface. The current density also remained significantly

larger up to at least +0.5 V_{SCE}. Observation of the scribed surface during the test showed that the current increase was accompanied by the formation of a green corrosion product along the length of the scratch. Thus, the scribing experiment confirmed that the spontaneous repassivation of a severely damaged film is unlikely at potentials more noble than -0.150 V_{SCE} (+0.092 V_{SHE}). This behaviour is very similar to that observed in chloride solution containing BTAH, where a limiting potential has been observed above which defective inhibiting films are incapable of spontaneous repair [1].

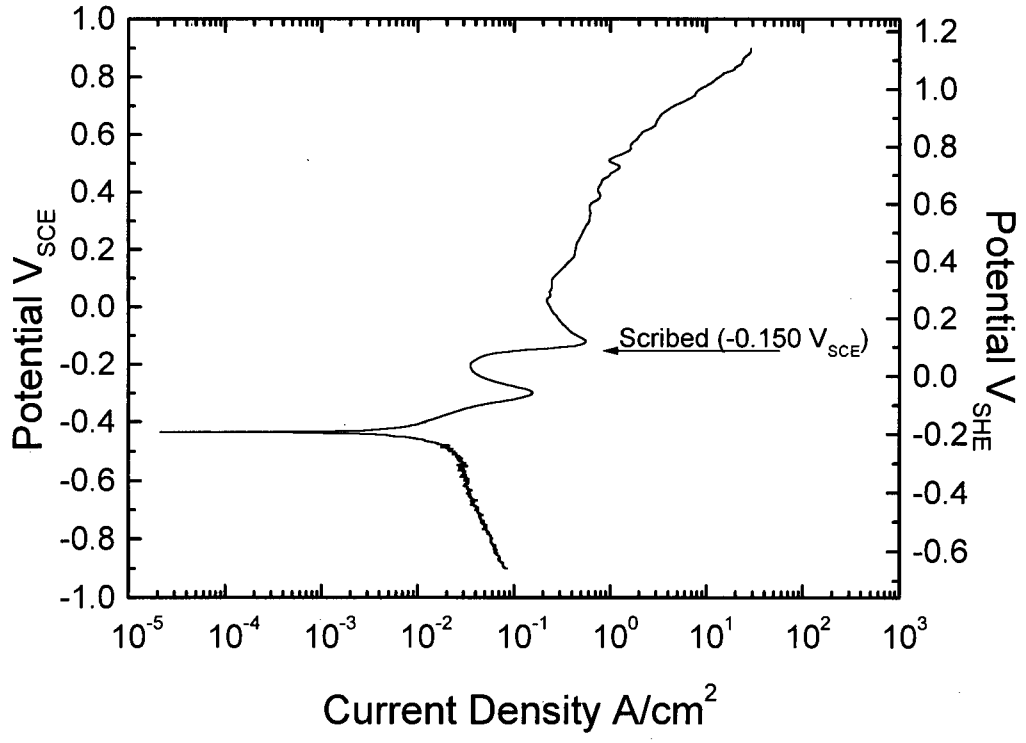

Figure 20 Scribing test on Cu in 1M NaBr containing 1.0 g/l BTAH at pH 6.0. Surface scribed at -0.150 V_{SCE}

It should be noted that the scribing test indicated that the formation of CuBr might prevent the reformation of damaged or defective inhibiting films. The equilibrium potential ($E_{CuBr/Cu}$) above which CuBr should form in the test solution is +0.040 V_{SCE} (see *Equation 10* and *Equation 11*). This potential was ~52 mV lower than the scribing potential, indicating that CuBr could have formed along the scratch during the scribing process, consistent with the visual observation of the formation of a green corrosion product.

Metallographic analysis of inhibitor films

Samples were prepared for metallographic examination in solutions containing BTAH as well as solutions containing no inhibitor. These samples were then examined under both an optical microscope and a scanning electron microscope (SEM).

There were no observable differences in surface structure when comparing samples created with and without inhibitors present, both under an optical microscope and under the SEM. The only noticeable difference was the samples prepared with the inhibitor would build a surface charge in the SEM, evidenced by a increase in brightness, in a shorter time than samples prepared without any inhibitor present.

Chapter 5 Discussion

Effect of molecular structure on inhibitor properties

The results from Figure 9 clearly demonstrate that the organic compounds benzotriazole (BTAH), and tolyltriazole (TTAH) are able to strongly inhibit the anodic dissolution of copper in solutions containing chlorides, under conditions where a clean copper surface exists with no intervening solid interlayer (i.e. a solid cuprous oxide or cuprous chloride surface layer). Both molecules exhibit very similar properties of inhibition and appear to operate by the same general mechanism.

The results also show that the organic compound methylbenzimidazole (MBM) does produce a significant inhibition of the anodic dissolution reaction, but not following the same mechanism and benzotriazole and tolyltriazole. The polarisation scans from experiments in solutions containing MBM show a decreased anodic current density in comparison to scans performed in inhibitor free solutions, but not as great a decrease as found with BTAH and TTAH, and also do not exhibit the current peak and subsequent current decrease associated with the formation of the protective polymeric film. This indicates that the MBM molecules are adsorbing onto the surface of the copper electrode, producing a barrier to diffusion, but not forming the copper-MBM complex necessary for the formation of the thicker inhibition films. These results confirm that substituting a carbon atom for a nitrogen atom in the molecules triazole group removes the ability to form the cuprous-organic complex that is required for the formation of the polymeric inhibition films, but does not prevent inhibition by an adsorbed monolayer. These results also demonstrate that the presence of a methyl group attached to the benzene ring of these organic molecules does not affect the formation of the copper-organic complex involved in inhibition.

The results also show that the onset of inhibition is slightly higher in potential for TTAH than it is for BTAH. Tromans & Sun [1] suggested that the onset of inhibition of was controlled by the potential of zero charge (PZC) where neutral organic molecules have the least "competition" diffusing to the working electrode surface from charged ions whose diffusion is potential driven. This suggests that the addition of the methyl group to the BTAH molecule to form TTAH alters the molecule's ability to diffuse to the Outer Helmholtz plane. This could be due to the methyl group causing the TTAH molecule to have a slightly polar orientation, thus altering the potential at which it most easily diffuses to the sample surface [30].

The degree of reduction of the current density in the region of inhibition was affected by the addition of the methyl group to BTAH. The decrease of the current density in the inhibition region was greater in the solutions containing BTAH than in solutions containing TTAH. Two separate explanations account for this observation. First, Tornkvist et al. [30] reported that the BTAH molecules show a clear tendency to have a flat rather than an edge orientation to the copper surface, whereas the TTAH molecular plane has an inclined orientation. This would result in BTAH molecules producing a greater area of diffusion barrier per molecule, or if the surface packing arrangement is equal for both TTAH and BTAH, the BTAH molecules would provide a greater degree of overlap, resulting in a more effective diffusion barrier.

However, Tornkvist et al. [30] also reported that the addition of the methyl group to BTAH to create TTAH resulted in the molecule being hydrophobic. Based on a single chemisorbed layer, this would result in TTAH being a more efficient inhibitor than BTAH. However, beyond the first chemisorbed monolayer, the hydrophobic nature of

TTAH will also act as a barrier towards the formation of thicker TTAH films, whereas BTAH would not suffer from the same barrier to further film growth, thus more easily producing inhibition films of greater thickness. Notoya and Poling [29] reported that TTAH formed much thinner films than BTAH and concluded that TTAH was not a "film-forming" inhibitor but rather an "adsorptive" inhibitor which did not grow beyond the first chemisorbed monolayer. Tornkvist et al. [30] confirmed that TTAH was present as a Cu-TTA complex present in the film in a polymeric structure, and Zhou et al [50] indicated that Cu-TTA films formed less rapidly than Cu-BTA.

Effect of scan rate on the inhibition properties of benzotriazole and tolyltriazole in chloride solutions

In an electrochemical reaction, a change in potential shifts the reaction away from steady state conditions. The reaction changes its rate and proceeds to shift towards a new steady state condition. With increasing time at the new potential the reaction will approach closer to the new steady state conditions for that potential.

In electrochemical polarisation scans the potential is stepped by a set amount in a specified time period, called a scan rate (e.g. 1 mV/s provides a 1 mV step every 1 second). In a polarisation scan the current measurement for that potential is taken at the end of the time step, prior to the potential being stepped to the next setting. The larger the potential step, the larger the deviation of the electrochemical reaction from steady state. Thus a slower scan rate results in the current measurements more closely reflecting the steady state conditions for the system. Therefore, comparing polarisation scans performed at different scan rates will identify which factors are more affected by a

movement away from steady state conditions. Typically effects which are dependent on diffusion are more widely affected by scan rate.

Effect on benzotriazole behaviour

The polarisation tests in Figure 10 show that the initial chemisorbtion reaction of the inhibition process occurs at potentials approximately 34 mV more negative with a reduction in scan rate from 1.0 to 0.2 mV/s. Tromans and Sun [1] reported that the growth of the inhibition film is diffusion dependent, and therefore time dependent. At the lower scan rate the diffusion and film growth would occur over a narrower range of potential, and is likely to be the cause of the slight reduction in potential.

The current peak indicating the onset of inhibition (i_p) was decreased in magnitude with a decrease in the scan rate from 0.1389 A/m^2 at 1 mV/s to 0.0253 A/m^2 at 0.2 mV/s. This decrease in current density with a decrease in scan rate was also likely to be caused by the longer time available for diffusion and growth of the inhibition film before increases in potential increased the rate of anodic dissolution of copper. These observations match well with the postulation that the film growth is self-limiting in behaviour, acting as a diffusion barrier to further growth and thickening.

Decreasing the polarisation scan rate from 1.0 mV/s to 0.2 mV/s raised the potential at which inhibition film breakdown occurred from 0.167 V_{SCE} to 0.875 V_{SCE} or higher. The decrease in scan rate increased the time available for nucleation and growth of the $(Cu\text{-}BTA)_n$ film on the surface before the sample reached higher potentials. The greater time available for film growth may have resulted in a more complete film growth

resulting in a decrease in the density of film defects. This would allow the film to provide more effective protection at higher potentials.

Effect on tolyltriazole behaviour

The polarisation studies in Figure 11 show that the initial process of inhibition occurs at a potential approximately 26 mV more negative at a 0.2 mV/s scan rate than at 1.0 mV/s. This suggests that the first limiting step of inhibition of the anodic dissolution involves diffusion of the TTAH molecules to the copper surface followed by chemisorbtion of TTAH on the copper surface, similar to the behaviour of BTAH inhibition. As with the results for BTAH, the current peak (i_p) indicating the onset of inhibition was reduced in magnitude from 0.0496 A/m^2 at a 1.0 mV/s scan rate to 0.0087 A/m^2 at 0.2 mV/s, also indicating that the growth of the TTAH inhibition film was time dependent.

Unlike the results observed with benzotriazole, the potential at which the TTAH inhibition film would breakdown was not affected by scan rate, occurring at approximately the same potential of 0.250 V_{SCE} regardless of the scan rate employed. This suggests that, while the mechanism of inhibition is the same as seen with BTAH, the structure and growth of the $(Cu\text{-}TTA)_n$ polymeric film differs from that of $(Cu\text{-}BTA)_n$.

Summary of the effect of scan rate on inhibition properties

The scan rate studies indicated that the formation of the initial inhibiting film is likely to occur by the same mechanism for both BTAH and TTAH. After the initial formation of the adsorbed monolayer, however, the behaviour changes, with BTAH providing protection to higher potentials with lower scan rates and TTAH protection

being potential dependent. These results suggest that the TTAH inhibition layer may consist of only the initial chemisorbed monolayer, as suggested by Notoya and Poling [29]. However, the potential dependence of the maximum current density (i_p) suggests that there is a period of film thickening and growth for the TTAH inhibition layer. Therefore, it is more likely that the TTAH inhibition film includes a polymeric $(Cu\text{-}TTA)_n$ film formed on the substrate of the chemisorbed monolayer. Support for this view comes from Tornkvist et al. [30] who confirmed the presence of the Cu-TTAH complex in the inhibition film. Zhou et al. [50] reported that TTAH films are much slower to grow than benzotriazole films, but that the films can grow to equal thicknesses. This conflicts with the reports by Notoya and Poling [29] who showed that TTAH produced inhibition films much thinner than BTAH.

In summary, it appears that tolyltriazole, like the benzotriazole, produces films that continue to grow after their initial formation, but at a slower rate, and reach a limit in thickness that is thinner than the benzotriazole films which are more resistant to breakdown at higher potentials.

Effect of inhibitor concentration on inhibition properties of benzotriazole and tolyltriazole in chloride solutions

Effect on benzotriazole behaviour

The polarisation studies in Figure 12 show that the potential at the current peak (i_p) increases +29mV with a decrease of BTAH concentration from 1.0 to 0.1 g/L. The potential change is small and is most likely due to the increase in the time necessary for film growth to occur, due to the decreased diffusion rate caused by the lower

concentration of BTAH in the bulk solution. The small effect of concentration change on the potential at i_p indicates that inhibition is not greatly affected by the rate of diffusion of the BTAH molecules from the bulk solution to the copper surface, but is controlled mainly by the thermodynamic condition (electrochemical potential) at the sample surface.

In the study by Tromans and Sun [1] it was suggested that the potential at which the chemisorbtion reaction occurred (*Equation 3*) was dictated by the Potential of Zero Charge (PZC) where the diffusion of a neutral organic molecule would receive the least competition from soluble ionic molecules whose diffusion would otherwise be driven by a differential in charge across the diffusion layer. The small shift in the potential at i_p that occurred with a change in inhibitor concentration indicates a set potential at which the chemisorbtion reaction occurs, after which the diffusion and time dependent film growth occurs. The small change observed in the potential at i_p is likely caused by the differences in film growth rates producing different time delays until the inhibition effect becomes detectable.

The maximum current density at the current peak (i_p) increases significantly with a decrease in BTAH concentration. This indicates that the rate of nucleation and growth of the $(Cu\text{-}BTA)_n$ film is dependent on the rate of diffusion of BTAH from the bulk solution to the sample surface . Thus the slower rate of diffusion causes a time delay in the thickening of the inhibition film allowing the polarisation scan to reach a higher potential, and thus a higher current density before a decrease in current density becomes noticeable.

The size of the decrease in the rate of anodic dissolution (i) that occurred above i_p was diminished with a decrease in BTAH concentration. This suggests that the structure of the polymeric inhibition film alters with changes in concentration, becoming a less effective diffusion barrier with decreasing concentration of BTAH in the bulk solution. For example, this could be a result of the structure of the polymeric film becoming more porous and less coherently formed with a lower BTAH concentration.

In solutions containing 0.1 g/L BTAH the potential where the inhibiting film was observed to breakdown occurred at a lower potential of -0.082 V_{SCE} compared with 0.167 V_{SCE} at a benzotriazole concentration of 1.0 g/L. This supports the view that the structure of the inhibiting film changes with concentration, becoming a less effective diffusion barrier when formed at lower concentrations.

Effect on tolyltriazole behaviour

The polarisation studies in Figure 13 show that the potential i_p rises 10 to 15 mV with a decrease of TTAH concentration from 1.114 g/L to 0.111 g/L. As with the BTAH results, this change is small and is possibly due to a lower concentration of TTAH in the bulk solution resulting in a slower growth rate of the inhibition film, delaying the point at which film growth produces a noticeable decrease of the anodic dissolution reaction. The slower growth rate of TTAH films, as compared to BTAH films, reported by Zhou et al. [50] suggests that the diffusion of TTAH molecules to the sample surface may not be the only limiting factor in the growth of the TTAH films. The hydrophobic nature of TTAH reported by Tornkvist et al. [30] might provide an additional barrier to film growth in addition to the diffusion effects. This would explain why the concentration dependent potential shift is smaller with TTAH than BTAH.

The thin nature of the TTAH films reported by Notoya and Poling [29], coupled with the slow reported growth rate, may prevent TTAH from forming a sufficiently thick barrier film to provide effective inhibition of the anodic dissolution of copper prior to breakdown at high potentials. This would explain the variability of TTAH being able to provide effective inhibition at a 0.111 g/L concentration, and suggests protection against a 1.0 mV/s change in potential requires a lower limiting concentration of 0.111 g/L.

For protective films formed with TTAH formed at 0.111 g/L TTAH, the potential at which the film breakdown occurs is the same as for films formed at higher TTAH concentration. This suggests that the final thickness of the TTAH film is not controlled by the concentration of the TTAH in the bulk solution, or the diffusion rate to the copper surface during film formation.

Summary of the effect of concentration changes on inhibition properties of benzotriazole and tolyltriazole in chloride solutions

The initial formation of the inhibition films are dependent on the thermodynamic condition of the sample surface, and both BTAH and TTAH films form initially by the same mechanism. The growth and thickening of the films also occur by the same mechanism but appear to be limited by different factors. The diffusion of BTAH to the sample surface and the diffusion of cuprous ions through the inhibitor film limit the growth of BTAH films. The growth of TTAH films appears to be limited by the hydrophobic characteristic of TTAH [30] presenting a barrier to further film growth.

Behaviour of copper in bromide solutions

The results have clearly demonstrated that copper exhibits a significant region of active behaviour in the presence of 1 M NaBr. Within the pH range investigated, there is very good agreement between the predicted behaviour based on the thermodynamics of the system and the observed polarisation behaviour. The thermodynamic analyses summarised in Figure 14 predict an active region in the near neutral to acid range of pH that is associated with the formation of stable cuprous bromide complexes. Consistent with this, an analysis of the slope and position of the apparent Tafel region of behaviour in Appendix 1 shows that anodic dissolution of copper in this region is controlled by the diffusion of $CuBr_2^-$ species from the metal surface. Additionally, this analysis provided a check on the chemical free energy of the aqueous $CuBr_2^-$ complex and suggested that the value may be closer to -194 kJ/mole than that listed in Table 3.

The stability's of cuprous bromide and cuprous chloride complexes are such that the E-pH diagrams of the $Cu\text{-}Cl^-\text{-}H_2O$ [1] and $Cu\text{-}Br\text{-}H_2O$ systems, and the anodic polarisation characteristics of copper in chloride [1,2,3,4,5,6,7] and bromide solutions of pH $\leq$ 7, are very similar. In fact the two systems are sufficiently comparable that anodic current oscillations that have been observed in acidic chloride media at potentiostatically controlled potentials near the anodic current peak and in the weakly passive current plateau region [2,51,52] should be observed under similar conditions in acidic bromide solutions. The oscillations in chloride environments have been attributed to the cyclic formation/dissolution of a CuCl film [1,51,52] and it is anticipated that a similar oscillation should be associated with the formation/dissolution of a CuBr film.

Adsorption of benzotriazole in bromide solutions

The polarisation studies in the presence of BTAH (Figure 18) clearly established that dissolution of copper was inhibited in the apparent Tafel region of active behaviour, confirming that the inhibitor interacted with the oxide-free copper surface under conditions where cuprous complexes were formed. This interaction (adsorption) was potential dependent, occurring most rapidly in a ~50 mV range of potentials between -0.300 and -0.250 V_{SCE} (approximately -0.06 to -0.01 V_{SHE}) in bromide solutions. The interaction potential showed no dependence on pH in tests conducted at pH 6.0 and 3.0, indicating that the initial adsorption reaction did not involve protons. For example, the neutral molecule BTAH is the most dominant and abundant soluble benzotriazole species in the pH range of the tests (see Table 1) and could be adsorbing directly on the copper surface according to *Equation 14*.

$$Cu + BTAH \rightarrow Cu(BTAH)_{ads} \qquad \textit{Equation 14}$$

Indirect support for a reaction such as that shown in *Equation 14* comes from the work of Thierry and Leygraf [34], who conducted in-situ surface-enhanced Raman scattering studies in aqueous chloride solutions containing benzotriazole over a range of potentials between -0.7 and -0.1 V_{SCE}. They concluded that benzotriazole is nondissociatively chemisorbed on copper, and it is reasonable to expect similar chemisorbtion in bromide solutions.

It is known that the cuprous benzotriazole compound, CuBTA (i.e. Cu^{+}-BTA^{-}), is very insoluble and is precipitated when BTAH is added to solutions of cuprous salts [17].

Thus, precipitation of CuBTA should occur in the active region by interaction between $CuBr_2^-$ species and BTAH, as shown in *Equation 15*.

$$CuBr_2^- + BTAH \rightarrow CuBTA + H^+ + 2Br^- \qquad \textit{Equation 15}$$

The formation of CuBTA via *Equation 15* should occur close to the metal surface where the concentration of the cuprous complex is highest, and its formation may be expected to play an important role in the overall corrosion inhibition process. However, it does not appear to be the first critical step because protons are involved in the reaction, whereas the interaction potential for inhibition is not pH dependent. Thus, a precursor step may be necessary such as *Equation 14*, which produces the initial adsorbed monolayer onto which the CuBTA would subsequently adsorb.

The potential at which benzotriazole interacts most rapidly with copper to promote anodic inhibition in the bromide solutions is only 50 to 100 mV lower than that of -0.200 V_{SCE} (~ +0.040 V_{SHE}) observed in chloride solutions [1]. These differences are not large and suggest that differences in halide species do not change the fundamental nature of the initial adsorption process. It was proposed by Tromans and Sun [1] that the rapid interaction at +0.040 V_{SHE} in chloride solutions was related to the potential of zero charge (PZC) of the copper electrode, as it is close to the PZC of +0.007 V_{SHE} reported by Rozenfeld [53] for copper in dilute chloride solutions. At the PZC, neutral molecules dissolved in the electrolyte are able to compete with soluble ionic (charged) species and adsorb more easily onto metal surfaces [53]. There was no information on the PZC of copper in bromide solution in the literature, but the review by Bertocci and Turner [54] suggests that the effects of Br^- and Cl^- on PZC values are similar. Consequently, it is

possible that the PZC also plays a dominant role in determining the potential at which rapid adsorption of the soluble neutral molecules of BTAH occurs in bromide solutions. This explains why *Equation 14* is most likely to represent the initial adsorption step.

The anodic inhibition process is expected to be completed by the formation of a layer of CuBTA, involving reactions of the type shown in *Equation 15*, that grows on the initial chemisorbed benzotriazole monolayer. Poling [19] showed that polymeric films of $(CuBTA)_n$ form in chloride solutions, and the structure of such films in halide and non-halide systems has been studied by several workers [17,36,38,55]. It is reasonable to expect that similar films form during the anodic inhibition in the bromide solution. The thickness of these films was not studied, but it must be less than the first-order interference thickness (ζ) because no surface colour changes or tarnishing effects were observed during anodic inhibition. ζ can be calculated by $\zeta = (\lambda / 4n)$ where λ is the wavelength of the visible spectrum of light undergoing interference and n is the refractive index of the film [56]. Brusic et al. [55] have shown that $n \approx 1.8$ for the polymeric film, so that based on a λ of ~450 nm for violet light the estimated value of ζ should be less than 62.5 nm. This value can be compared with the ellipsometry studies of Brusic et al. [55] on $(CuBTA)_n$ polymer films on copper in halide free sulphate solutions, where the thickness was 3 to 4 nm at pH 7.0 and became thicker and more poorly formed as the pH decreased. A poorly formed film at lower pH values is consistent with the higher observed passive current density in bromide solution at pH 3.0 relative to pH 6.0 (refer to Figure 18 and Figure 19).). The studies of Brusic et al. [55] indicate that poorly formed, less protective $(CuBTA)_n$ films have a lower degree of polymerisation and exhibit more "patchy growth," the latter being related to nucleation factors. Therefore, it is possible

that the higher passive currents observed at pH 3.0 relative to pH 6.0 in the present work are related to structural differences in $(CuBTA)_n$ polymer films. A structural dependence on pH suggests that protons are involved in reaction governing nucleation and/or growth of the polymeric films. Protons are produced during formation of CuBTA via *Equation 15* suggesting that film formation based on this reaction is hindered at lower pH values, consistent with the effects of pH on passive current densities in Figure 18 and Figure 19.

Spontaneous repair of damaged inhibitor films

The scribing test (Figure 20) indicated that damaged or defective inhibiting films are unlikely to undergo spontaneous repair at potentials more noble than -0.150 V_{SCE} (+0.092 V_{SHE}). This behaviour may be explained if the first critical step in the inhibition (repassivation) process is the adsorption of BTAH onto the copper surface (*Equation 14*) and that BTAH is prevented from reaching the metal surface at potentials where the film damage occurs. It was noted earlier that *Equation 10* and *Equation 11* show that it is thermodynamically possible for CuBr to form on the exposed copper surface if the film is damaged above +0.040 V_{SHE}. Therefore, the presence of CuBr may be sufficient to prevent BTAH from interacting with the copper surface. Another process hindering repassivation, previously proposed to account for similar behaviour in chloride containing solutions [1] and applicable to the present study, is related to mass transfer effects. The simple mass transfer model developed in this earlier study [1] is based on the interaction between a flux of cuprous halide complexes ($CuBr_2^-$) diffusing from a freshly exposed copper surface and the opposing flux of BTAH species diffusing from the bulk solution toward the copper surface. The model shows that precipitation of CuBTA in the diffusion layer will probably prevent any BTAH from reaching the copper surface when

the concentration of cuprous complexes at the outer Helmholtz plane (OHP) exceeds the concentration of BTAH in the bulk solution. Approximating concentrations to activities, the analysis predicts an approximate limiting condition for film repair that is based ion the equality of activities shown in *Equation 16*.

$$\left[CuBr_2^-\right]_{OHP} \cong \left[BTAH\right]_{bulk} \qquad \textit{Equation 16}$$

The activity of the cuprous complex at the OHP is given by *Equation 7* as discussed in the Appendix. Hence, at the limiting potential above which damaged films are unable to spontaneously repair is obtained by substituting $[BTAH]_{bulk}$ for $[CuBr_2^-]$ in *Equation 7*. In the present study where $[BTAH]_{bulk}$ is ~8.4×10^{-3} and $[Br^-]$ is 0.7, the limiting potential becomes +0.091 V_{SHE} (-0.151 V_{SCE}), which is the same as that observed experimentally. The agreement is probably closer than the model merits, but it does indicate that mass transfer and precipitation effects in the diffusion layer are capable of limiting the repair of damaged inhibiting films by preventing any BTAH molecules from reaching and adsorbing onto the copper surface.

Discussion of metallographic studies

In a scanning electron microscope a sample will, over a period of time, build a surface charge caused by the samples inability to conduct the electrons bombarding the sample surface to earth. The surface charging is evidenced in an electron microscope by the sample surface increasing in brightness. Samples which posses a greater conductivity are able to conduct the charge away at a greater rate, and therefore exhibit a slower rate of increasing brightness. The test sample prepared in the chloride-BTAH solution exhibited a much faster rate of increase in surface brightness compared to a sample

prepared in the absence of BTAH. This is consistent with the presence of the inhibiting $(Cu\text{-}BTA)_n$ film reducing the conductivity of the sample surface, confirming the presence of the polymeric film.

The samples prepared in the presence and absence of BTAH showed no observable differences when viewed under an optical microscope. The lack of coloration on sample with the inhibition film presence shows that the inhibition film did not grow beyond the first-order interference thickness (ζ). As described earlier ζ can be calculated by $\zeta = (\lambda / 4n)$ where λ is the wavelength of visible light and n is the refractive index of the film [56]. Using the value $n \approx 1.8$ shown by Brusic et al. [55] for the polymeric film and $\lambda \approx 450$ nm for violet light, the thickness of the film must be less than 62.5 nm.

As the only observable difference in the SEM between the samples prepared in the presence and absence of BTAH was the rate of surface charging it can be assumed that the thickness of the inhibitor film is less than the observed resolution of the SEM. This can be calculated by $R = (L / Mag) \bullet 1 / x$ where R is the resolution of the SEM, L = 10 cm is the length of the electron micrograph, Mag = 2000 is the magnification of the electron micrograph, and x = 1000 is the number of scan lines in the micrograph. This produces a resolution limit of 50 nm. This result shows good agreement with the results of the optical microscopy evaluation.

Chapter 6 Conclusions

Anodic polarisation studies of copper behaviour in 1M NaCl in the pH range 3 <7 in the presence and absence of benzotriazole, tolyltriazole and methylbenzimidazole are consistent with the following conclusions.

1. Disrupting the tri-nitrogen group of the azole structure of the organic molecules prevents the formation of the cuprous-organic complex necessary for forming the chemisorbed polymeric inhibition film. Adding a methyl group to the benzene ring does not disrupt the formation of the cuprous-organic complex.

2. Tolyltriazole is an effective inhibitor for the anodic dissolution reaction for copper, utilising the same general mechanism of inhibition as benzotriazole.

3. The hydroscopic nature of tolyltriazole prevents thickening of tolyltriazole inhibition films, resulting in a less protective films compared to benzotriazole.

4. The results here are in agreement with the inhibition model proposed by Tromans and Sun [1].

Theoretical analyses of potential-pH equilibria in the Cu-Br^--H_2O system, together with anodic polarisation studies of copper behaviour in 1M NaBr in the pH range ≥ 3 <7 in the presence and absence of 1.0 g/litre benzotriazole (BTAH) inhibitor, are consistent with the following conclusions.

1. The formation of aqueous cuprous bromide complexes, $CuBr_2^-$, affects the stability of both copper and copper oxide and promotes active dissolution behaviour of copper, similar to that observed in chloride solutions.

2. The active region exhibits an apparent Tafel behaviour with characteristics that are consistent with anodic dissolution being controlled by mass transport of cuprous bromide species, similar the effect of cuprous chloride complexes in chloride solutions. A detailed analysis of the apparent Tafel region indicates that it may be used to check the value of the chemical free energy of the cuprous halide complex.

3. Adsorption and interaction of benzotriazole on oxide free copper surfaces leading to corrosion inhibition is potential dependent. It occurs most rapidly in the active region over the potential range -0.060 to -0.010 V_{SHE} where the anodic dissolution products are cuprous bromide complexes. The results suggest that the first step in the formation of a benzotriazole containing corrosion inhibiting film involves the adsorption of the neutral molecule, BTAH. Inhibition is less effective at lower pH values.

4. A scribing test indicates that there is an upper limiting potential above which damaged corrosion inhibiting benzotriazole films are unlikely to undergo spontaneous repair. Thermodynamic and mass transfer considerations suggest that this potential is controlled either by formation of CuBr on the exposed copper surface or the precipitation of a CuBTA salt in the diffusion layer so that BTAH molecules are prevented from reaching and interacting with the copper surface.

References

[1] D. Tromans & R. Sun, Journal of the Electrochemical Society, Vol. 138, pg. 3235 (1991)

[2] R.S. Cooper & J.H. Bartlett, Journal of the Electrochemical Society, Vol. 105, pg. 109, (1958)

[2] A.L. Bacarella & J.C. Griess Jr., Journal of the Electrochemical Society, Vol. 120, pg. 459 (1973)

[4] M. Braun & K. Nobe, Journal of the Electrochemical Society, Vol. 126, pg. 1666 (1979)

[5] W.H. Smyrl, in "Comprehensive Treatise of Electrochemistry," Vol.4, J. Bockris, B.E. Conway, E. Yeager, H.P. Lee & K. Nobe, Journal of the Electrochemical Society, Vol. 133, pg. 2035 (1986) & R.E. White, Editors, pg. 97-149, Plenum Press, New York (1981)

[6] H.P. Lee & K. Nobe, Journal of the Electrochemical Society, Vol. 133, pg. 2035 (1986)

[7] O.E. Barcia, O.R. Mattos, N. Pebere & B. Tribollet, Journal of the Electrochemical Society, Vol. 140, pg. 2825 (1993)

[8] H.E. Barner & R.V. Scheurmen, Handbook of Thermodynamic Data for Compounds and Aqueous Species, John Wiley & Sons, Inc., New York (1978)

[9] D.D. Wagman, W.H. Evans, V.B. Parker, R.H. Schumm, I. Halow, S.M. Bailey, K.L. Churney, and R.L. Nuttall, The NBS Tables of Chemical Thermodynamic Properties: Selected Values for Inorganic and C1 and C2 Organic Substances in SI Units, Journal of Physics & Chemistry Reference Data, Vol. 11, Supplemental No. 2 (1982); published by the American Chemical Society and the American Institute of Physics for the National Bureau of Standards

[10] U. Bertocci & D.D. Wagman, in Standard Potentials in Aqueous Solutions, A.J. Bard, R. Parsons, and J. Jordan, Editors, pg. 287-293, IUPAC, Marcel Dekker, Inc., New York (1985)

[11] F.D. Rossini, D.D. Wagman, W.H. Evans, S. Levine, and I. Jaffe, Selected Values of Chemical Thermodynamic Properties, NBS Circular 500, U.S. Department of Commerce, National Bureau of Standards, U.S. Printing Office, Washington, DC (1952)

[12] W.M. Latimer, The Oxidation States of the Elements and their Potentials in Aqueous Solutions, 2nd Edition, Prentice-Hall, Inc., Englewood Cliffs, NJ (1952)

[13] L.G. Sillen & A.E. Martell, Stability Constants of Metal-Ion Complexes, Special Publication No. 17, The Chemical Society, London (1964)

[14] F. Mansfeld, T. Smith, & E. P. Parry, Corrosion, Vol. 27, pg. 289 (1971)

[15] R. Walker, Journal of the Electrochemical Society, Vol. 29, pg. 290 (1973)

[16] I. Dugdale & J. B. Cotton, Corrosion Science, Vol. 3, pg. 69 (1963)

[17] J. B. Cotton & I. R. Scholes, British Corrosion Journal, Vol. 2, pg. 1 (1967)

[18] D. Altura & K. Nobe, Corrosion, Vol. 28, pg. 345 (1972)

[19] G. W. Poling, Corrosion Science, Vol. 10, pg. 359 (1970)

[20] I. C. G. Ogle & G. W. Poling, Canadian Metallurigical Quarterly, Vol. 14, pg. 37 (1975)

[21] P. G. Fox, G. Lewis, & P. J. Boden, Corrosion Science, Vol. 19, pg. 457 (1979)

[22] F. El-Taib Heakal & S. Haruyama, Journal of the Electrochemical Society, Vol. 20, pg. 887 (1980)

[23] J. S. Wu & K. Nobe, Corrosion, Vol. 37, pg. 223 (1981)

[24] W. Shen & K. Nobe, in Surfaces, Inhibition, and Passivation, (PV 86-7) E. McCafferty & R. J. Brodd, Editors, pg. 82, The Electrochemical Society Softbound Proceedings Series, Pennington, NJ (1986)

[25] R. Youda, H. Nishihara & K. Aramaki, Eletrochimica Acta, Vol. 35, pg. 1011 (1990)

[26] L. Angely, M. Bonnemay, G. Bronoel & G. Peslerbe, Metaux, pg. 409 (1971)

[27] F. Mansfeld & T. Smith, Corrosion, Vol. 29, pg. 105 (1973)

[28] J. Fagel & G. W. Ewing, Journal of the American Chemical Society, Vol. 73, pg. 4360 (1951)

[29] T. Notoya & G. W. Poling, Journal of the Electrochemical Society, Vol. 35, pg. 193 (1979)

[30] C. Tornkvist, D. Thierry, J. Bergmann, B. Liedberg & C. Leygraf, Journal of the Electrochemical Soceity, Vol. 136, pg. 58 (1989)

[31] D. Chadwick & T. Hashemi, Corrosion Science, Vol. 18, pg. 39 (1978)

[32] T. Hashemi & C. A. Hogarth, Eletrochimica Acta, Vol. 33, pg. 1123 (1988)

[33] J. J. Kester, T. E. Furtak & A. J. Bevolo, Journal of the Electrochemical Society, Vol. 129, pg. 1716 (1982)

[34] D. Thierry & C. Leygraf, Journal of the Electrochemical Society, Vol. 132, pg. 1009 (1985)

[35] R. Youda, H. Nishihara & K. Aramaki, Corrosion Science, Vol. 28, pg. 87 (1988)

[36] B. F. Roberts, Journal of Electron Spectroscopy & Related Phenomenon, Vol. 4, pg. 273 (1974)

[37] Bo-Shung Fang, C. G. Olson & D. W. Lynch, Surface Science, Vol. 176, pg. 476 (1986)

[38] J. O. Nilsson, C. Tornkvist & B. Liedberg, Applied Surface Science, Vol. 37, pg. 306 (1989)

[39] D. Tromans & R. Sun, Journal of the Electrochemical Society, Vol. 139, pg. 1945 (1992)

[40] Handbook of Chemistry and Physics, 70th Edition, R.C. Weast, D. Lide, M. Astle, & W. Beyer, Editors, pg. D-254, CRC Press Inc., West Palm Beach, FL (1990)

[41] M. Pourbaix, Atlas of Electrochemical Equilibria, Pergamon Press Inc., New York (1966)

[42] M. Pourbaix, in Localized Corrosion, B. F. Brown, J. Kruger, & R. W. Staehle, Editors, pg. 12-32, NACE, Houston, Texas (1974)

[43] R. Bartonicek & M. Lukasovska, Corrosion Science, Vol. 9, pg. 35 (1969)

[44] R. Bartonicek & M. Lukasovska, Corrosion Science, Vol. 11, pg. 111 (1971)

[45] G. Bianchi & P. Longhi, Corrosion Science, Vol. 13, pg. 853 (1973)

[46] U. Bertocci & D. R. Turner, in Encyclopedia of Electrochemistry of the Elements, Vol. II, A. J. Bard, Editor, pg. 383-484, Marcel Dekker Inc., New York (1974)

[47] Standard Potentials in Aqueous Solutions, A. J. Bar, R. Parsons & J. Jordan, Editors, Marcel Dekker Inc., New York (1985)

[48] Handbook of Chemistry and Physics, 70th Edition, R. C. Weast, D. Lide, M. Astle & W. Beyer, Editors, pg. D-172, CRC Press Inc., West Palm Beach, FL (1990)

[49] N. V. Sedgwick, The Chemical Elements and Their Compounds, Vol. I, pg. 119-121, Oxford University Press, London (1950)

[50] G. D. Zhou, Z. Ma, R. Tong, & T. Notoya, Bull. Electrochem., Vol. 7, pg. 60 (1991)

[51] H. P. Lee, K. Nobe & A. J. Pearlstein, Journal of the Electrochemical Society, Vol. 132, pg. 1031 (1985)

[52] M. R. Bassett & J. L. Hudson, Journal of the Electrochemical Society, Vol. 137, pg. 1815 (1990)

[53] I. L. Rozenfeld, Corrosion Inhibitors, pg. 115-119, McGraw-Hill Inc., New York (1981)

[54] U. Bertocci & D. R. Turner, in Encyclopedia of Electrochemistry of the Elements, Vol. II, A. J. Bard, Editor, pg. 383-484, Marcel Dekker Inc., New York (1974)

[55] V. Brusic, M. A. Frisch, B. N. Eldridge, F. P. Novak, F. B. Kaufman, B. M. Rush &G. S. Frankel, Journal of the Electrochemical Society, Vol. 138, pg. 2253 (1991)

[56] O. Kubaschewski & B. E. Hopkins, Oxidation of Metals, 2nd edition, pg. 182-190, Butterworth and Co. Ltd., London (1962)

[57] K. J. Vetter, Electrochemical Kinetics, pg. 189-190, Academic Press Inc., New York (1967)

Appendix

Anodic exchange current densities of cuprous halide complexes are believed to be relatively high. For example, the review by Bertocci and Turner [54] reports estimated values to be of the order of 10 to 100 A/m^2 in solutions containing 0.1 M of Cu^I. Consequently, the anodic dissolution of copper in the active region in Figure 17 is very likely to be under the diffusion controlled transport of $CuBr_2^-$ from the metal surface, similar to the process that has been proposed for the behaviour of copper in chloride solutions [1,3,5,6,7]. Furthermore, provided there is a sufficiently large excess of supporting electrolyte, such as 1 M NaBr in the present study, the effect of the potential gradient on the electrical migration of cuprous species becomes negligible [5]. In this case the transport of the cuprous species is controlled mainly by the concentration (activity) gradient of the species in solution. Thus, the one dimensional flux (j) of $CuBr_2^-$ ions diffusing into the bulk solution from the OHP may be expressed simply in terms of the diffusion coefficient (D) and the concentration gradient (dc/dx), as shown in *Equation 17*.

$$j_{CuBr_2^-} = -\left(D_{CuBr_2^-}\right)\bullet\left(\frac{dc}{dx}\right)_{CuBr_2^-} \text{, mol/m}^2\text{s} \qquad \textit{Equation 17}$$

where x is measured from the OHP and normal to the electrode surface, and the concentration is in units of mol/m^3. At steady state, the concentration gradient is dependent only on the concentrations of the species at the OHP and in the bulk solution so that *Equation 17* becomes

$$j_{CuBr_2^-} = \left(\frac{D_{CuBr_2^-}}{\delta}\right)\left\{\left(CuBr_2^-\right)_{OHP} - \left(CuBr_2^-\right)_{bulk}\right. \text{, mol/m}^2\text{s} \qquad \textit{Equation 18}$$

where δ is the diffusion layer thickness.

In practice, the concentration of the cuprous complex in the bulk solution will be negligibly small in relation to that at the OHP and a further simplification may be made to the flux equation

$$j_{CuBr_2^-} = \left(\frac{D_{CuBr_2^-}}{\delta}\right)\left(CuBr_2^-\right)_{OHP} \text{ , mol/m}^2\text{s} \qquad \textit{Equation 19}$$

Hence the anodic current density (i) becomes

$$i = F \bullet j_{CuBr_2^-} \approx \left(\frac{F \bullet D_{CuBr_2^-}}{\delta}\right)\left(CuBr_2^-\right)_{OHP} \text{ , A/m}^2 \qquad \textit{Equation 20}$$

where F is the Faraday constant 9.6519 x 10^4 C.

The concentration of the complex in *Equation 20* is related to its activity so that at low concentrations $(CuBr_2^-)_{OHP} = [CuBr_2^-]_{OHP}$ x 10^3 mole/m^3, and *Equation 20* becomes

$$i = F \bullet j_{CuBr_2^-} \approx \left(\frac{F \bullet D_{CuBr_2^-}}{\delta}\right)\left(\left[CuBr_2^-\right]_{OHP} \times 10^3\right) \text{ , A/m}^2 \qquad \textit{Equation 21}$$

At any potential E at 25 °C (298 K), the logarithm of the equilibrium activity of $[CuBr_2^-]_{OHP}$ may be obtained from *Equation 7* by substituting $E = E_{CuBr_2^- / Cu}$ and rearranging

$$\log\left[CuBr_2^-\right]_{OHP} = 2\log\left[Br^-\right] + \left(\frac{E - 0.195}{0.059}\right) \qquad \textit{Equation 22}$$

Therefore, taking the logarithms of *Equation 21*, and substituting for log[$CuBr_2^-$]$_{OHP}$ from *Equation 22*, the following relationship between E and log i is obtained

$$E \approx 0.059 \log i - 0.118 \log[Br^-] - 0.059 \log\left(\frac{F \bullet D_{CuBr_2^-}}{\delta}\right) + 0.018 \text{ , } V_{SHE} \quad \textit{Equation 23}$$

It is readily evident from *Equation 23* that dE/d log i is 59 mV for constant values of [Br^-], δ, and $D_{CuBr_2^-}$. This is consistent with the value of the apparent Tafel slope in the active region of Figure 17.

The general validity of *Equation 23* may be assessed further by substituting values for the variables [Br^-], δ, $D_{CuBr_2^-}$ that are relevant to the present study and computing the final equation that defines the active region in Figure 17. The experiments were conducted under the same conditions used previously [39] where stirring produced laminar flow parallel to the working electrode surface at 50 mm/s and for which delta was estimated to be 1.34 x 10^{-4} m, based on laminar flow relationships [57]. Also, [Br^-] = 0.7 and $D_{CuBr_2^-}$ = 1.18 x 10^{-9} m^2/s [17]. Substitution of these values into *Equation 23* leads to the relationship

$$E \approx 0.059 \log i + 0.040 \text{ , } V_{SHE} \qquad \textit{Equation 24}$$

Consequently, when i = 1 A/m^2, *Equation 24* predicts that E will be +0.040 V_{SHE} (-0.206 V_{SCE}). This compares fairly well with the observed value of -0.266 V_{SCE} in Figure 17. The major source of the ~60 mV discrepancy between *Equation 24* and the observed behaviour is unlikely to be due to a significant error in the estimation of δ,

because its dependence on fluid velocity (v) is proportional to $(v)^{-1/2}$ [57]. The discrepancy is most probably associated with uncertainty in the chemical free energy (G°) of the $CuBr_2^-$ species listed in Table 3. . For example, if the listed value is in error by ~5 kJ/mole so that the corrected $G^\circ_{CuBr_2^-}$ is ~ -194 kJ/mole, $E^\circ_{CuBr_2^-}$ becomes +0.144 VSHE, instead of +0.195 V_{SHE} (see *Equation 7*), and *Equation 24* becomes

$$E = 0.059 \log i - 0.011 \text{ , } V_{SHE} \qquad \textit{Equation 25}$$

which is closer to the observed behaviour. Interestingly, this suggests that careful analysis of the active region of copper behaviour in the presence of halide may be a useful technique for obtaining good estimates of the chemical free energy of cuprous halide complexes. Such careful analyses should be conducted with a rotating disk electrode [57] because it allows greater control of the diffusion layer thickness required for insertion into *Equation 23*.